A role for EP3 and its associated G protein, G_z, in negatively regulating beta-cell function and mass in the context of insulin resistance and obesity.

Austin Reuter[1,2], Jaclyn A. Wisinski[1,2], Darby Peter[1,2], Michael D. Schaid[1,3], Rachel J. Fenske[1,3], and Michelle E. Kimple[1,2,3,4,5]*

1, Research Service, William S. Middleton Memorial VA Hospital, Madison, WI, 53705.
2, Department of Medicine, Division of Endocrinology, Diabetes, and Metabolism, 3, Interdepartmental Graduate Program in Nutritional Sciences, 4, Department of Academic Affairs, and 5, Department of Cell and Regenerative Biology, University of Wisconsin-Madison, Madison, WI, 53705.

*Corresponding Author
Michelle E. Kimple, PhD
Research Health Scientist
William S. Middleton Memorial VA Hospital

Associate Professor of Medicine, Division of Endocrinology, Diabetes, and Metabolism
Director of the Basic Science Selective, Department of Academic Affairs
Faculty Affiliate, Department of Cell and Regenerative Biology
University of Wisconsin School of Medicine and Public Health

4148 UW Medical Foundation Centennial Building
1685 Highland Ave.
Madison, WI 53705

608-265-5627
mkimple@medicine.wisc.edu

Abstract

Objective: Black and Tan Brachyury (BTBR) mice have underlying defects in insulin sensitivity and beta-cell function, even when lean. When homozygous for the *Leptin^{Ob}* mutation (BTBR-Ob), hyperphagia leads to morbid obesity, and by 10 weeks of age, a type 2 diabetes (T2D) phenotype is fully penetrant. The second messenger molecule, cyclic AMP (cAMP), promotes glucose-stimulated and incretin-potentiated insulin secretion, beta-cell proliferation, and beta-cell survival. We have previously shown that a key player in the loss of functional beta-cell mass in the BTBR-Ob strain is Prostaglandin EP3 receptor (EP3); dysfunctionally up-regulated in the islet by the pathophysiological conditions of T2D. EP3 transmits a signal from its ligand, prostaglandin E2 (PGE_2), to the unique cAMP-inhibitory G protein alpha-subunit, $G\alpha_z$, reducing beta-cell cAMP production. Our objective in this study was to study the effect of beta-cell EP3 and $G\alpha_z$ loss on the metabolic phenotype of both BTBR-lean and -Ob mice, providing support for targeting this pathway in a genetically-susceptible population before and after the progression to frank T2D.
Methods: EP3 or $G\alpha_z$-floxed BTBR mice were bred with BTBR mice expressing Cre recombinase under the control of the rat insulin promoter in order to design beta-cell-specific knockout mice. A final cross into the BTBR-Ob strain provided both lean and obese experimental animals. To our surprise, the EP3 deleted allele was transferred via the germline, making full-body EP3-null mice, as confirmed by qPCR. Beta-cell-specific $G\alpha_z$ loss in $G\alpha_z$-flox-RIP-Cre mice ($G\alpha_z$ βKO) was confirmed; yet, these mice were poor breeders, particularly in the context of the *Leptin^{Ob}* mutation; therefore, only BTBR-lean mice were phenotyped. Full-body metabolic and ex vivo islet assays were conducted in wild-type and EP3-null BTBR-lean and Ob mice and wild-type and $G\alpha_z$ βKO BTBR-lean mice, linking any islet phenotype with observed effects on glucose homeostasis.
Results: Systemic EP3 loss accelerated the early T2D phenotype of BTBR-Ob mice and caused insulin resistance and glucose intolerance in BTBR-lean mice, likely due to the extra-pancreatic effects described previously in other mouse models. Even so, islets from EP3-null BTBR-Ob mice had significantly increased insulin-positive pancreas area, supportive of an increased proliferation response. $G\alpha_z$ βKO BTBR-lean mice, on the other hand, had significantly improved glucose tolerance due to elevated glucose-stimulated and incretin-potentiated insulin secretion, with no apparent effect of beta-cell $G\alpha_z$ loss on beta-cell proliferation. Combined, our findings suggest a divergence in signaling downstream of EP3/$G\alpha_z$ depending on the (patho)physiologic conditions to which the islet is exposed.
Conclusions: Our work sheds light on G protein-mediated mechanisms by which beta-cells compensate for systemic insulin resistance and how these become dysfunctional in the T2D state.

Keywords: EP3 receptor; G protein signaling; insulin secretion, beta-cell compensation; prostaglandin E_2; signal transduction

Introduction

Type 2 diabetes mellitus (T2D) occurs after a failure of the insulin-secreting pancreatic beta-cells to compensate for peripheral insulin resistance and its often-associated glucolipotoxic and inflammatory conditions. Underlying defects in both beta-cell function and the ability of the beta-cells to increase and maintain their mass are key factors in the susceptibility to T2D and can be genetically encoded. The Black and Tan Brachyury (BTBR) mouse is an excellent mouse model to mimic the natural course of T2D development in susceptible individuals. As a strain characteristic, BTBR mice are more insulin resistant than the more commonly used C57BL/6 sub-strains[1], but their T2D susceptibility is beta-cell centric. The BTBR strain has an underlying deficit in insulin granule exocytosis[2, 3], and, coupled with a failure of BTBR mice homozygous for the *Leptin*^{Ob} mutation (BTBR-Ob) to up-regulate an islet cell cycle gene module early in the compensation response[4, 5], BTBR-Ob mice rapidly and reproducibly develop severe obesity and insulin resistance, ultimately succumbing to frank T2D by 10 weeks of age[1].

The second messenger molecule, cyclic AMP (cAMP), has been well-characterized as a potentiator of glucose-stimulated insulin secretion (GSIS), and has been linked with the compensatory functional, proliferative and survival responses to insulin resistance, glucolipotoxicity, and inflammation. A multitude of changes in the beta-cell highly compensating for insulin resistance converge on the conservation of cAMP levels, including up-regulation of signaling mediated by cAMP-stimulatory G_s-coupled G protein coupled receptors (GPCRs) (e.g., the glucagon-like peptide 1 receptor: GLP1R), down-regulation of signaling mediated by cAMP-inhibitory G_i-coupled GPCRs (e.g., the somatostatin receptors: SSTRs), and altered expression and activity of cAMP-degrading phosphodiesterase enzymes. Islets from T2D BTBR-Ob mice have a deficit in the ability to increase cAMP production in response various stimuli; an effect correlated with reduced glucose-stimulated and incretin-potentiated insulin secretion [6]. Prostaglandin EP3 receptor (EP3) is a G_i-coupled receptor for E series prostaglandins such as prostaglandin E_2 (PGE_2): its most abundant natural ligand. Islets from BTBR-Ob mice and T2D human organ express more EP3 and produce more PGE2 than islets from lean and/or non-diabetic controls, suggesting that up-regulation of PGE_2-mediated EP3 signaling is a dysfunctional consequence of the T2D condition itself that might be able to be therapeutically targeted. In support of this concept, when islets isolated from BTBR-Ob mice and T2D human organ donors are treated with the specific EP3 receptor antagonist, L798,106, their insulin secretion response to glucose and GLP1R agonists is at least partially restored [6].

In previous work from our laboratory using INS-1 (832/13) rat insulinoma cells and islets isolated from T2D C57BL/6J-Ob mice, we demonstrated beta-cell EP3 is specifically coupled to the unique G_i subfamily member, G_z[7, 8]. The catalytic alpha subunit of G_z, $G\alpha_z$, has many unique biochemical properties, including an extremely slow deactivation rate, meaning that it has the potential for partial tonic activity. $G\alpha_z$ tissue distribution is also quite limited, with protein only being found in brain, platelets, retina, and islets. $G\alpha_z$ is an important endogenous regulator of beta-cell cAMP production, as islets from $G\alpha_z$-null Balb/c mice produce more cAMP and secrete more insulin in response to glucose, consistent with reduced fasting glucose levels and accelerated glucose tolerance [9]. $G\alpha_z$-null mice are resistant to diabetes in a number of

mouse models of the disease. In T1D models, $G\alpha_z$-null mice display increased insulin secretion in reponse to glucose and the GLP1R agonist, exendin-4, an accelerated beta-cell replication rate, and improved beta-cell survival [10, 11). Of direct relevance to this work, when fed a high-fat diet, Gαz-null C57BL/6N mice are protected from glucose intolerance due to a significant enhancement of beta-cell replication and mass, increasing the insulin secretory capacity of the islet {Kimple, 2012 #7]. Considering beta-cell EP3 acts specifically through $G\alpha_z$, HFD-fed EP3-null mice should phenocopy the protection from glucose intolerance observed with $G\alpha_z$-null mice. Yet, in contrast to $G\alpha_z$, EP3 is highly expressed in other tissues, including white adipose tissue, where it limits lipolysis via G_z-independent mechanisms. Therefore, EP3-null mice become more dyslipidemic, insulin resistant, and, ultimately, glucose intolerant than wild-type controls [12]. Even so, when islets are isolated from HFD-fed EP3-null mice and studied *ex vivo*, their proliferative rate is significantly higher than those of wild-type HFD-fed controls, supporting the concept that if beta-cell EP3 could be specifically targeted, these mice would exhibit the same T2D protective phenotype of $G\alpha_z$-null mice [12].

In this work, we aimed to confirm the beta-cell autonomy of the protective phenotype of $G\alpha_z$-null mice against T2D, and validate beta-cell EP3 as a putative target for beta-cell-targeted therapies in T2D-susceptible individuals by generating beta-cell-specific $G\alpha_z$- and EP3-null mice in the BTBR background, recording effects on metabolic phenotype in both lean and genetically obese mice. Challenges in generating and breeding the mouse models necessitated a change in approach, and, ultimately, we were able to determine the *in vivo* metabolic and *ex vivo* islet phenotype of full-body EP3-null mice in the BTBR-lean and -Ob backgrounds, as well as that of beta-cell-specific $G\alpha_z$-null mice in the BTBR-lean background. Combined, our results lend support to targeting beta-cell $G\alpha_z$ signaling as a therapeutic strategy to improve glucose tolerance, particularly in a T2D-susceptible population.

Materials & Methods

Materials and Reagents

Sodium chloride (S9888), potassium chloride (P3911), magnesium sulfate heptahydrate (M9397), potassium phosphate monobasic (P0662), sodium bicarbonate (S6014), HEPES (H3375), calcium chloride dehydrate (C3881), exendin-4 (E7144) and RIA-grade bovine serum albumin (A7888) were purchased from Sigma Aldrich (St. Louis, MO, USA). Anti-insulin antibodies (Insulin + Proinsulin Antibody, 10R-I136a; Insulin + Proinsulin Antibody, biotinylated, 61E-I136bBT) were from Fitzgerald Industries (Acton, MA, USA). The 10 ng/ml insulin standard (8013-K) and assay buffer (AB-PHK) were from Millipore. RPMI 1640 medium (11879–020: no glucose), penicillin/streptomycin (15070–063), and fetal bovine serum (12306C: qualified, heat inactivated, USDA-approved regions) were from Life Technologies (Carlsbad, CA, USA). Dextrose (D14–500) was from Fisher Scientific (Waltham, MA). Humulin R® was from Eli Lilly and Co. Guinea pig anti-insulin, antibody diluent with background reduction, EnVision™ diaminobenzidine (DAB) reagents, and and serum-free blocking agent were from Dako. Superfrost® Plus microscope slides were from Fisher Scientific (Hampton, NH, USA), and fluorescence quality 1.5-mm coverslips were from Corning Life Sciences (Lowell, MA, USA). The rat/mouse insulin ELISA kit was from Crystal Chem Inc. (Downers Grove, IL, USA). Glucose

Oxidase Reagent was from Pierce. The RNeasy Mini Kit and RNase-free DNase set were from Qiagen. High-Capacity cDNA Reverse Transcription Kit was from Applied Biosystems. FastStart Universal SYBR Green Master mix was from Roche.

Mouse husbandry

Breeding colonies were housed in a limited-access, pathogen-free facility where all cages, enrichment, and water were sterilized before use (University of Wisconsin-Madison, Biotron) on a 12-hour light/12-hour dark cycle with *ad libitum* access to water and irradiated breeder chow (Teklad 2919).

Upon weaning, mice were housed five or fewer per cage of mixed genotypes with ad libitum access to lower-fat chow in the Madison VA Animal Resource Facility (LabDiet 5001, nonirradiated). All procedures were performed according to approved protocols in accordance with the principles and guidelines established by the University of Wisconsin and Madison VA institutional animal care and use committees.

Mouse model generation and validation

C57BL/6J mice in which Cre expression is driven by the rat insulin promoter (RIP-Cre^{Herr}: "InsPr-Cre" in [13]) were obtained from Pedro Herrera as described in [11]. As compared to other RIP-Cre driver lines, RIP-Cre^{Herr} shows the least hypothalamic Cre expression and does not contain the human growth hormone minigene, which has been shown in previous studies to produce full-length, active hGH that artificially enhances mouse beta-cell proliferation through the prolactin receptor[14].

B6/129 mice in which the first coding exon of the *Ptger3* gene is flanked by LoxP sites (EP3-floxed) were obtained from The Jackson Laboratory (*Ptger3*^{tm1Csml}; stock 008349, deposited by Michael Lazarus). These mice were bred with RIP-Cre^{Herr} to generate a mixed-background EP3-flox-RIP-Cre mouse, which was then backcrossed into the BTBR *T+ Itpr3*^{tf}/J (BTBR) background more than 10 generations by Alan Attie's group at UW-Madison to generate the EP3-flox-RIP-Cre BTBR strain. In order to transfer the EP3-flox-RIP-Cre BTBR colony to our SPF breeding core, founder mice were re-derived from clean embryos implanted into pseudopregnant BTBR females. As a strain characteristic, the outcome of in vitro fertilization in the BTBR background is quite poor[15], and only four live pups were born, with only one containing the floxed allele (see Table 1 for genotyping primer sequences). This mouse was bred with BTBR mice ordered from The Jackson Laboratories to increase colony size, and then a final cross was performed with BTBR.Cg-Lepob/WiscJ heterozygous for *Lep*^{Ob} to generate the EP3-flox-RIP-Cre BTBR-Ob colony. Experimental mice were generated by breeding EP3-flox$^{+/-}$Ob$^{+/-}$Cre$^{-/-}$ animals with EP3-flox$^{+/-}$Ob$^{+/-}$Cre$^{+/-}$ animals.

During the course of our study, and to reconcile disparate results, we designed genotyping primers to detect the deleted alleles in tail tissue samples (a full list of genotyping primer sequences can be found in Table 1). In every case, only the wild-type or deleted allele was detected, independent of Cre expression (Supplemental Figure 1A). Upon re-genotyping of tail DNA from the single founder mouse, only the deleted allele was detected, indicating germline

transmission of the mutation. To confirm our EP3-flox-RIP-Cre mice were actually full-body knockouts, we performed qPCR on adipose and kidney RNA samples (chosen because of high endogenous EP3 expression), and found no amplification of *Ptger3* PCR product in knock-out tissues (Supplemental Figure 1B,C) (no antibody exists that specifically detects EP3 protein, whether endogenous or over-expressed).

The generation and tissue-specific validation of the $G\alpha_z$-flox-RIP-Cre line in the C57BL/6J background has been described previously [11]. These mice were backcrossed into the BTBR background more than 10 generations, with a final cross into BTBR-Ob to generate the $G\alpha_z$-flox-RIP-Cre BTBR-Ob line. Experimental mice were generated by breeding $G\alpha_z$-flox$^{+/-}$Ob$^{+/-}$Cre$^{-/-}$ animals with $G\alpha_z$-flox$^{+/-}$Ob$^{+/-}$Cre$^{+/-}$ animals. As with the EP3-null mice described above, $G\alpha_z$-flox-RIP-Cre BTBR mice, whether in the BTBR background or C57BL/6J background, were similarly genotyped for the deleted allele, which was observed occasionally in genotyping reactions (Supplemental Figure 2A,B). All $G\alpha_z$-flox-RIP-Cre experimental mice described in this and our previous manuscript [11] are confirmed to be beta-cell-specific $G\alpha_z$-null, with no deleted allele detected upon tail tissue genotyping[1]. Genotyping primer sequences are listed in Table 1.

In certain experiments, we also utilized full-body $G\alpha_z$-null mice the BTBR background, which were generated from a previously-described and validated $G\alpha_z$-null C57BL/6N line by backcrossing into the BTBR background more than 10 times [7].

Mouse metabolic phenotyping and tissue collection

Except for BTBR-lean and BTBR-Ob females being lighter than males at 6 weeks of age, and BTBR-lean females lighter than males at 8 weeks of age, no differences in random-fed blood glucose or 4-6 h fasting blood glucose levels were observed as a sex characteristic (Supplemental Figure 3A-C). Therefore, in BTBR studies, both male and female mice were used.

Oral glucose tolerance tests (OGTTs) were performed at 6 weeks of age after a 4-6 h fast in clean cages. 1 mg/kg sterile dextrose solution was administered via gavage needle at 6 weeks of age, with blood glucose levels recorded at various timepoints by blood glucose meter (AlphaTRAK) and rat/mouse–specific test strips reading of a blood droplet obtained via tail nick, as previously described[10, 16, 17]. The OGTT on $G\alpha_z$-flox-RIP-Cre mice in the C57BL/6J background was performed similarly, except that mice were 10-week-old males. In some cases, blood was collected in EDTA-coated microcapillary tubes at baseline and 5 or 15 min after glucose injection to generate plasma samples for insulin assay. Insulin tolerance tests (ITTs) were performed similarly to OGTTs, except that 0.75 mg/kg Humulin-R was IP injected. As BTBR mice regularly have a glucose spike after insulin injection, the percent change in blood glucose was normalized to the blood glucose level 5 min after insulin injection. Mice were sacrificed

[1] Based on our extensive experience with genotyping $G\alpha_z$-flox-RIP-Cre mice in the NOD, C57BL/6J, and BTBR backgrounds, the germline transmission of the deleted allele appears related to the underlying insulin sensitivity of the mouse strain, as tail samples from $G\alpha_z$-flox-RIP-Cre NOD mice (a highly insulin sensitive strain) amplify the deleted allele at a rate of 0.65% of total alleles genotyped; $G\alpha_z$-flox-RIP-Cre C57BL/6J mice at a rate of 3.88%; and BTBR (an insulin resistant strain) at a rate of 5.38%. This may be an important factor for researchers to consider when making beta-cell-specific knockout mice using any constitutive Cre reporter strain.

between 9 and 10 weeks of age for terminal islet, blood, or tissue collection. To isolate pancreatic islets, mice were anesthetized by 2,2,2 tribromoethanol until unresponsive, exsanguinated by cutting the descending aorta, and the bile duct ligated and cannulated, followed by injection of ice-cold collagenase solution to inflate the pancreas as described previously[18]. For terminal blood collection in order to generate plasma samples, mice were fasted 4-6 h in clean cages and anesthetized by 2,2,2 tribromoethanol until unresponsive, and mice were exsanguinated by retro-orbital puncture with an EDTA-coated microcapillary tube, followed by secondary euthanasia by cervical dislocation. Whole pancreases were harvested upon necropsy and fixed in formalin at 4 degrees C overnight, and then cryo-preserved.

Pancreas section histochemical staining and insulin immunohistochemistry

Hematoxylin and eosin staining (for islet morphology) and insulin immunohistochemistry with hematoxylin counterstain (for measurement of beta-cell fractional area) were performed as previously described for paraffin-embedded pancreas sections [7, 10, 11]. Adipose tissue and kidney were harvested upon necropsy and flash-frozen in liquid nitrogen for future isolation of total RNA. GSIS assays were performed using a single-islet microplate GSIS assay, and total islet insulin content and secreted insulin quantified via an in-house sandwich ELISA as previously described[19].

Plasma insulin, glucose, and PGE metabolite measurements

The insulin concentration of 4-6 h fasting plasma samples and plasma samples from OGTTs was determined using a Crystal Chem high-sensitivity insulin ELISA as previously described[11]. Plasma glucose was recorded via Pierce glucose oxidase assay according to the manufacturers' directions. Plasma PGE metabolite concentrations were determined by PGE metabolite EIA according to the manufacturer's protocol, as previously described[6, 17].

Ex vivo islet insulin secretion and cAMP production assays

Mouse islets were purified from exocrine tissue of inflated pancreases using collagenase digestion and centrifugation through Histopaq as previously described[20]. Isolated human islets were obtained from the Integrated Islet Distribution Program (IIDP) between 2013 and 2015. Single-islet GSIS assays were performed with the indicated compounds using tissue-culture-treated 96-well V-bottom dishes as previously described[19].

Quantitative PCR assays

150-200 islets from each mouse islet preparation were washed with PBS and used to generate RNA samples via Qiagen RNeasy Mini Kit according to the manufacturer's protocol. Copy DNA (cDNA) was generated and relative qPCR performed via SYBR Green assay using primers validated to provide linear results upon increasing concentrations of cDNA template, as previously described[11]. A list of qPCR primer sequences can be found in Table 2.

Statistical analysis

Data are expressed as mean ± standard error of the mean (SEM) unless otherwise noted. Data were analyzed as appropriate for the experimental design and as indicated in the text and

figure legends. P-values < 0.05 were considered statistically significant. Statistical analyses were performed with GraphPad Prism version 7 (GraphPad Software, San Diego, CA).

Results

Full-body EP3 loss may accelerate the early T2D phenotype of BTBR-Ob mice. We generated mice lacking $G\alpha_z$ specifically in the beta-cells in the BTBR-lean and BTBR-Ob backgrounds in order to test the impact of beta-cell $G\alpha_z$ loss on metabolic parameters in the healthy and T2D state. The penetrance of $G\alpha_z$-flox-RIP-Cre mice was lower than the expected Mendelian ratio in both the lean and Ob background, but particularly so in the Ob background. Therefore, completing a full metabolic characterization of beta-cell-specific $G\alpha_z$ loss in the BTBR-Ob background became prohibitively expensive. Therefore, we focused solely on characterizing the impact of full-body EP3 loss in the BTBR-Ob background.

At 6 weeks of age, there were no significant differences in mean body weight between wild-type and EP3-null BTBR-Ob mice (Fig. 1A) (while the weights of all mice were included in the analysis, those suspected of low weight due to end-stage T2D are indicated in grey circles). There were also no significant differences in mean random-fed blood glucose levels between the groups (Fig. 1B) (blood glucose levels above the range of the glucometer—750 mg/dl—also suggesting end-stage T2D, were recorded as 750 mg/dl and are indicated by grey circles). Mice not suspected of end-stage T2D were fasted 4-6 h before performing OGTTs, and, per our approved animal protocol, if a fasting blood glucose measurement exceeded 450 mg/dl (indicating little functional beta-cell mass), mice were excluded from OGTT. Although the 4-6 h fasting blood glucose levels of mice excluded from OGTT were not recorded, 50% of wild-type BTBR-Ob mice (7 of 14) and 70% of EP3-null BTBR-Ob mice (7 of 10) were excluded from OGTT, suggesting the EP3-null mutation accelerated T2D development in the BTBR-Ob strain. Among those mice subjected to OGTT, there were no significant differences in mean 4-6 h fasting blood glucose levels or glucose tolerance between EP3-null and wild-type BTBR-Ob mice, with both groups displaying fasting hyperglycemia (mean 4-6 h fasting blood glucose levels ≈ 325-375 mg/dl) and severe glucose intolerance (peak blood glucose levels ≈ 550-600 mg/dl) (Fig. 1C,D).

At 8 weeks of age, when insulin tolerance tests were performed, there were no differences in body weight of BTBR-Ob mice by genotype (Fig. 1E). Similar to OGTTs, mice were fasted for 4-6 h prior to insulin tolerance tests. Neither mean random-fed blood glucose levels nor 4-6 h fasting blood glucose levels were significantly different between groups as a factor of genotype (Fig. 1F,G). Both wild-type and EP3-null BTBR-Ob mice were severely insulin resistant, with zero effect of insulin on reducing blood glucose levels at any time point after insulin injection (Fig. 1H). Combined, these results indicate that, although EP3-null BTBR-Ob mice may have had a stronger T2D phenotype at 6 weeks of age, by 8 weeks of age, there was no additional impact of EP3 loss on the BTBR-Ob T2D phenotype.

Full-body EP3 loss and beta-cell-specific $G\alpha_z$ loss have opposing effects on the early metabolic phenotype of BTBR-lean mice. In order to confirm the $G\alpha_z$-floxed mutation had no impact on metabolic parameters of interest, allowing direct comparisons between EP3-null and $G\alpha_z$-floxed-RIP-Cre mice to the same wild-type control group, we performed a pilot study with wild-

type Cre-negative, wild-type Cre-positive, and $G\alpha_z$-floxed Cre-negative mice at 6 weeks of age. There was no effect of the $G\alpha_z$-floxed mutation on body weight or 4-6 h fasting blood glucose as compared to either control group (Supplemental Figure 4A-C), and the mean OGTT curves nearly overlaid each other (Supplemental Figure 4G). Similar results were found with ITTs performed at 8 weeks of age (Supplemental Figure 4D-F,H).

At 6 weeks of age, there were no significant differences in body weight among wild-type, EP3-null, or $G\alpha_z$-flox-RIP-Cre BTBR-lean mice (Fig. 2A), and after a 4-6 h fast, there were no significant differences in blood glucose levels (Fig. 2B). Upon oral glucose challenge, EP3-null BTBR-lean mice had significantly delayed glucose clearance as compared to wild-type controls, with significantly higher blood glucose levels 30 and 45 min after glucose challenge as compared to wild-type lean controls and a 2-3-fold higher mean 2 h glucose area-under-the-curve (8819 ± 3694 mg/dl glucose, EP3-null BTBR-lean vs. 5612 ± 1966 mg/dl glucose, wild-type BTBR-lean; mean ± SEM) (Fig. 2C). In contrast, the glucose clearance of $G\alpha_z$-flox-RIP-Cre mice was accelerated as compared to wild-type controls, with significantly lower blood glucose levels 15, 30, and 45 min after glucose challenge (Fig. 2C). The effect of beta-cell-specific $G\alpha_z$ loss is strain-specific, as both the fasting blood glucose and oral glucose tolerance of 10-week-old wild-type and beta-cell-specific $G\alpha_z$-null male mice in the C57BL/6J background are nearly identical (Supplemental Figure 5A,B). Finally, data from a separate cohort of 10-week-old $G\alpha_z$-flox-RIP-Cre BTBR-lean mice and wild-type Cre-positive controls revealed no significant differences in body weight, 4-6 h fasting plasma glucose, 4-6 h fasting plasma insulin, or islet insulin content by genotype, supportive of a lack of effect of the $G\alpha_z$-null mutation on GSIS in the BTBR-lean mice in the absence of glucose/incretin stimulation (Supplemental Figure 5D-F).

Consistent with their decreased glucose tolerance, 8-week-old EP3-null BTBR-lean mice had significantly reduced insulin sensitivity as compared to wild-type controls, with significantly elevated blood glucose levels 60 and 120 min after insulin injection, and a 1.5-fold decrement in 2 h glucose area-under-the curve in response to insulin (2946 ± 765.9 mg/dl glucose, EP3-null BTBR-lean vs. 4668 ± 698.5 mg/dl glucose, wild-type BTBR-lean; mean ± SEM) (Fig. 3C). This decreased insulin sensitivity was in the absence of any effect of the EP3-null mutation on body weight or 4-6 h FBG at 8 weeks of age (Fig. 3A,B). We did not perform a full ITT characterization in $G\alpha_z$-flox-RIP-Cre mice, as full-body $G\alpha_z$ loss has never been shown to have any impact on insulin sensitivity in any mouse model, consistent with the lack of $G\alpha_z$ expression in liver, adipose tissue, and skeletal muscle. Yet, one $G\alpha_z$-flox-RIP-Cre mouse subjected to ITT exhibited a similar decrement in blood glucose after insulin injection as those in any of the control groups (Supplemental Fig. 6).

<u>EP3 loss increases beta-cell fractional area of BTBR-Ob mouse pancreas sections.</u> Between 9 and 10 weeks of age, pancreases were collected from wild-type and EP3-null BTBR mice, both lean and obese, and fixed for paraffin-embedding and sectioning. Hematoxylin and eosin (H&E) staining of pancreas sections from 9-10-week-old BTBR-Ob mice, whether wild-type or EP3-null, revealed a clear destruction of normal, spherical, mouse islet architecture in many wild-type and EP3-null BTBR-Ob pancreas sections, with a number of elongated, poorly circumscribed islets and islet remnants near pancreatic ducts observed (Fig. 4A-F: example islets are circled in

red, with arrowheads indicating those considered to have poor morphology). Insulin IHC was performed on pancreas sections from both lean and obese wild-type and EP3-null BTBR mice counterstained with hematoxylin to calculate fractional beta-cell area (see representative images in Fig. 5A-D). Although the mean insulin positive pancreas area trended towards being greater in islets from wild-type BTBR-Ob mice as compared to lean at 9-10 weeks of age, this difference was not statistically significant (Fig. 5E). Interestingly, though, the insulin-positive pancreas area of EP3-null BTBR-Ob mice was significantly enhanced as compared to their lean controls. Although beta-cell replication was not specifically measured in our study, this result is consistent with the increased beta-cell replication rate of EP3-null mice fed a high-fat diet as compared to wild-type controls [12].

Islets were isolated from wild-type and EP3-null mice, both lean and obese, and subjected to single-islet GSIS assays in response to low glucose (2.8 mM), high glucose (16.7 mM), and high glucose plus 10 nM exendin-4 (Ex-4): an agonist for the GLP1R, which signals through a stimulatory G_s protein to augment cAMP production. GSIS was recorded as the total insulin secreted per islet in 45 min, normalized or not to the total islet insulin content. Statistical analyses were performed in both datasets; yet, normalizing secreted insulin to islet insulin content produced the most distinguishing results. Islets isolated from wild-type BTBR-lean mice secreted more insulin in response to 16.7 mM glucose than 2.8 mM glucose, whether reported as percent secreted or total secreted (Fig. 6A,B, grey vs. white bars). Adding Ex-4 had no additional effect on wild-type BTBR-lean islet GSIS (Fig. 6A,B, black vs. grey bars). Islets isolated from lean EP3-null mice had basally elevated GSIS, secreting over 50 times more glucose as a percent of content than wild-type BTBR-lean mice in 2.8 mM glucose, with no additional effect of 16.7 mM glucose (Fig. 6A, gray vs. white bars); yet, on average, secreted more insulin as a percent of content in response to Ex-4 (Fig. 6A, black vs. gray bars). In order to better compare the GSIS response of wild-type and EP3-null BTBR islets to stimulatory glucose and Ex-4, the stimulation index (SI) was calculated by the ratio of GSIS as a percent of content in 16.7 mM glucose to that in 2.8 mM glucose for each islet, while the incretin response (IR) was similarly calculated by normalizing GSIS as a percent of content in 16.7 mM glucose plus Ex-4 to that in 16.7 mM glucose alone. Islets from wild-type BTBR-lean mice had a mean SI of approximately 4.5, vs. approximately 1 for those from EP3-null BTBR-lean mice (Fig. 6C, white vs. light gray bars). Conversely, islets from wild-type BTBR-lean mice had a mean IR of approximately 1, while those from EP3-null BTBR-lean islets had an IR of approximately 1.5 (Fig. 6D, white vs. light gray bars).

Islets from both EP3-null and wild-type BTBR-Ob mice had elevated GSIS in low glucose (both ≈ 15-20-fold above that in wild-type BTBR-lean islets) (Fig. 6A,B) and responded more strongly to high glucose than low (SI ≈ 2) (Fig. 6C); yet, only islets from wild-type BTBR-Ob mice responded to Ex-4 to potentiate GSIS (IR ≈ 2.2) (Fig. 6D). Both BTBR-Ob groups had significantly lower insulin content than wild-type BTBR-lean mice, consistent with their hyperglycemia (Fig. 6E). Interestingly, though, islet insulin content was reduced in islets from both EP3-null BTBR-lean and BTBR-Ob mice as compared to their wild-type controls, consistent with an insulin hypersecretion phenotype (Fig. 6E).

Beta-cell loss of $G\alpha_z$ improves BTBR-lean islet function and incretin responsiveness.
As mentioned previously, our experimental cohort of $G\alpha_z$-flox-RIP-Cre mice was limited due to challenges in breeding; therefore, we were only able to complete islet GSIS assays from one 9-10-week old $G\alpha_z$-null-RIP-Cre mouse. Yet, as our GSIS assays are performed on single islets, and individual islets from the same animal are biologically distinct. Similar to the results described above for our wild-type vs. EP3-null BTBR-lean islet assays, islets from a wild-type Cre-positive control secreted significantly more insulin in response to stimulatory glucose than low glucose, with Ex-4 having no addition effect on GSIS, as represented by total insulin secreted in 45 min (Fig. 7A, black bars). In contrast, islets from a mouse lacking $G\alpha_z$ specifically in the beta-cells had no change in GSIS in response to stimulatory glucose as compared to those from lean controls, yet had a strong potentiation of GSIS with the addition of Ex-4 (Fig. 7A, grey bars). Islets from the $G\alpha_z$-flox-RIP-Cre mouse had a much higher SI than those from the wild-type Cre-positive control; yet, this effect was due almost exclusively to a lower secretion of insulin in basal glucose (Fig. 7B). The incretin response of islets from the $G\alpha_z$-flox-RIP-Cre mouse was approximately 1.5, vs. 1 for islets from the wild-type Cre-positive control (Fig. 7C). Unfortunately, we were not able to normalize secreted insulin to percent of islet insulin content, as this insulin ELISA failed due to a technical error. Yet, the lack of a difference in mean islet insulin content in a separate cohort of wild-type and $G\alpha_z$-floxed Cre-positive BTBR-lean mice (Supplemental Figure 5D) supports any differences in insulin secretion in response to various stimuli being due to a direct effect on secretion and not as due to a secondary effect on insulin content.

A potential defect in BTBR islet proliferation and relevance to $G\alpha_z$.
While all of our ex vivo islet assays, combined with our previous results from full-body $G\alpha_z$-null mice in young, lean backgrounds are supportive of an effect of loss of EP3/$G\alpha_z$ signaling on insulin secretion and not beta-cell mass, a failure of BTBR-Ob islets to up-regulate key cell cycle genes as compared to those from euglycemic C57BL/6J-Ob mice has been previously published[5]. By qCPR, FoxM1 and its target genes cyclin A2 (*Ccna2*), cyclin B1 (*Ccnb1*), cyclin-dependent kinase 1a/P21 (*Cdkn1a*) cyclin-dependent kinase 1b/p27 (*Cdkn1b*), *Nek2*, polo-like kinase 1 (*Plk1*), aurora kinase B (*Aurkb*), and centromere protein A (*CenpA*) were all significantly up-regulated (2-4-fold) in islets isolated from 10-week-old B6-lean vs. B6-Ob mice, but showed little-to-no change in islets isolated from BTBR-lean as compared to BTBR-Ob[4]. Thus, expression of FoxM1 and its targets predicts the metabolic phenotype of BTBR-Ob vs. B6-Ob mice[4]. We used a publicly-available microarray database of islet gene expression in C57BL/6J and BTBR mice, both lean and *Leptin*^{Ob}, at 4 and 10 weeks of age (diabetes.wisc.edu, [5]), to search for expression changes in key cell cycle genes between islets isolated from lean C57BL/6J and BTBR mice at both ages. In contrast to the results described above for C57BL/6J-Ob vs. BTBR-Ob mice, there was little difference among the relative gene expression of FoxM1 or any of its targets in islets from lean mice, whether from animals 4 or 10 weeks of age (Fig. 8A,B). Exceptions were *Ccna2*, which was ~50% higher in BTBR-lean islets as compared to C57BL/6J at 4 weeks of age, and *Cdkn1a*, which was ~15% higher in islets from BTBR-lean mice as compared to C57BL/6J at 10 weeks of age. Thus, an underlying defect in FoxM1 transcriptional regulation does not appear responsible for the phenotype of islets from BTBR lean mice.

Next, we looked at expression levels of a panel of other cell-cycle genes: ki67 (*mki67*), cyclin D2 (*Ccnd2*), cyclin-dependent kinase 2a (*Cdkn2a*), cyclin A1 (*Ccna1*), and cyclin D1 (*Ccnd1*). Again, there were few significant changes in gene expression observed (Fig. 8C,D). At 4 weeks of age, *mki67* abundance was increased approximately two-fold in islets isolated from BTBR-lean mice as compared to C57BL/6J-lean mice; this difference had disappeared by 10 weeks of age. In islets isolated from 10-week-old BTBR-lean mice, *Ccnd1* expression was enhanced ~20% as compared to islets from C57BL/6J mice. Yet, the strongest and most consistent change between BTBR and C57BL/6J islet expression of any of the cell cycle genes probed was cyclin D1 (*Ccnd1*), whose expression was approximately 3-fold lower in islets isolated from lean BTBR mice as compared to C57BL/6J mice, at both 4 and 10 weeks of age.

Cyclin D1 expression is absolutely required for the G1-to-S transition of the cell cycle, and its expression can be stimulated by activation of the cAMP-response element binding protein (CREB) transcription factor. To determine a potential impact of $G\alpha_z$ loss on BTBR-lean islet proliferation as a contributor to their improved glucose tolerance, we isolated islets from 10-week-old C57BL/6J-lean mice and wild-type or $G\alpha_z$-null BTBR-lean mice, purified RNA, and generated cDNA samples for qPCR. Although the mean cycle time is reduced in BTBR-lean mice as compared to B6-lean, this difference is not statistically-significant (by calculating relative mRNA expression using $2^{\Delta\Delta Ct}$, expression of cyclin D1 mRNA is reduced, on average, 12-fold in wild-type BTBR-lean mice as compared to B6-lean). In comparing the mean mRNA expression normalized to β-actin of $G\alpha_z$-null BTBR-lean islets as compared to wild-type BTBR-lean, we did not find a significant enhancement of *Ccnd1* expression when islet $G\alpha_z$ is lost, and relative *Ccnd1* abundance was only increased approximately 2-fold as compared to BTBR-lean (Fig. 9). Therefore, we conclude that loss of islet $G\alpha_z$ and enhancement of cAMP production does not have a significant impact on cyclin D1 expression, at least in young, lean BTBR mice, further supporting a secretion-centric model of the mechanisms behind $G\alpha_z$ loss on enhanced glucose tolerance of BTBR-lean mice.

<u>Mouse islet EP3 mRNA expression is correlated with insulin resistance and T2D status: differential expression of the constitutively-active EP3γ variant in the BTBR strain.</u>

Neither islets from C57BL/6N, C57BL/6J, nor BTBR mice respond to the EP3 agonists PGE_1 or sulprostone to reduce insulin secretion[6, 7, 10, 17]. Yet, islets isolated from T2D C57BL/6J-Ob and BTBR-Ob mice have a strong inhibitory GSIS response to EP3 agonists[6, 7, 17]. In the case of BTBR-Ob mice, islet expression of the gene encoding EP3, *Ptger3*, is up-regulated over 400-fold as compared to that of islets from BTBR-lean mice[6]. In theory, this argues against the EP3 receptor as playing a role in the secretion defect of BTBR-lean mice. Yet, a direct comparison of islet Ptger3 expression between the B6 and BTBR strains, whether lean or obese, has never been performed. qPCR for *Ptger3* using a primer set that detects all three mouse EP3 splice variants (α, β, and γ) using islet cDNA samples from C57BL/6N, C57BL/6J, non-diabetic C57BL/6J-Ob, T2D C57BL/6J-Ob, BTBR lean, and BTBR-Ob mice demonstrates a 90-fold up-regulation of islet *Ptger3* in T2D C57BL/6J-Ob as compared islets from lean C57BL/6N mice, and a 400-fold upregulation in islets from T2D BTBR-Ob mice as compared to C57BL/6N (Fig. 10A).

Interestingly, *Ptger3* expression was up-regulated approximately 6-fold in islets from BTBR-lean mice as compared to islets isolated from lean C57BL/6N mice.

Of the mouse EP3 splice variants, EP3ɣ is constitutively-active, meaning it signals to $G\alpha_z$ in an agonist-independent manner [21, 22]. Quantitative PCR using primers specific for mRNA of the EP3ɣ splice variant revealed a 43.3-fold increase in EP3ɣ mRNA in islets from BTBR-lean mice as compared to C57BL/6N, and a 1024-fold increase in BTBR-Ob islets (Fig. 10B).

Discussion

The central role of the beta-cell in the progression to T2D can be found in a number of population studies. Women who develop gestational diabetes have up to a 70% risk of developing T2D later in life, even if they are lean and normoglycemic before pregnancy [23]. As pregnancy is an insulin-resistant state, just as often associated with obesity or aging, the insulin secretory capacity must increase in order to maintain euglycemia[24]. The strong link between gestational diabetes and T2D later in life supports an underlying beta-cell defect being genetically encoded. More support for an underlying beta-cell defect as contributing to T2D comes from studies on individuals from the Pima Indian tribe, who have a high lifetime risk of developing T2D, twin studies, and studies of lean, normoglycemic individuals of two parents with T2D. While skeletal muscle insulin resistance has been identified as the primary defect in these populations, the progression to T2D is dependent on the beta-cell [25-29]. The BTBR strain used in this study is an excellent model of the natural course of T2D in a genetically-susceptible population. BTBR mice are more insulin resistant than C57BL/6 substrains, as measured by adipocyte glucose uptake or hyperinsulinemic-euglycemic clamp[1]. Lean BTBR mice have fasting hyperinsulinemia and elevated plasma C-peptide levels as compared to B6 mice[1]. Yet, BTBR islets secrete less insulin in response to glucose *ex vivo*[6]. In essence, BTBR beta-cells are working harder than those of B6 mice to maintain euglycemia, even when lean. Yet, even in the background of an underlying genetic susceptibility, if beta-cells continue to be able to maintain high function and mount a compensatory increase in mass, euglycemia will persist. The beta-cell compensates for the chronic pathophysiological changes of obesity and/or insulin resistance through adaptive metabolic, functional, proliferative, and survival mechanisms. Many of the signaling pathways used converge on maintaining or increasing beta-cell cAMP levels, highlighting the critical role of cAMP in the beta-cell adaptive response.

PGE_2, an eicosanoid derived from arachidonic acid incorporated into plasma membrane phospholipids, is the most abundant natural ligand for the EP3 receptor. High glucose, free fatty acids, and/or pro-inflammatory cytokines all have been shown to upregulate enzymes involved in the PGE_2 synthetic pathway—most notably, the rate-limiting enzyme, cyclooxygenase 2 or Cox-2 (a.k.a. prostaglandin-endoperoxidase synthase 2: Ptgs2). Culturing islets isolated from lean BTBR mice in conditions mimicking a glucolipotoxic environment—high glucose, palmitate, and pro-inflammatory cytokines—significantly up-regulates Cox-2 expression and PGE_2 production [17]. The sequentially increasing insulin resistance in 10-12 week-old C57BL/6N mice, 35-40-week-old C57BL/6N mice fed a low-fat control diet for 25-29 weeks, and 35-40-week old C57BL/6N mice fed a HFD for 25-29 weeks is directly correlated with their plasma PGE

metabolite levels [7], suggesting PGE_2-mediated EP3 signaling may contribute to the beta-cell pathology of pre-diabetes. Yet, islets isolated from non-diabetic mice or human organ donors have no functional response to either EP3 agonists or antagonists[8, 12, 17]. It is not until islets have been exposed to the frank T2D state that islet EP3 expression is significantly enhanced [6, 17]. Recent work from our laboratory using a panel of islets isolated from non-diabetic human organ donors of varying BMI reveals that enhanced COX-2 mRNA expression is correlated with significantly elevated islet insulin content, as well as with the expression of the pro-survival factor IL-6[30]. These results suggest that islet PGE_2 signaling may be an important contributor to the beta-cell compensatory response.

Islets isolated from T2D mice and humans exhibit significantly elevated PGE_2 production and EP3 expression as compared to islets from lean and/or non-diabetic controls, and treatment with an EP3 antagonist, L798,106, augments their GSIS response[6]. These findings suggest EP3 actively contributes to beta-cell dysfunction and loss of functional beta-cell mass in T2D. In the beta-cell, EP3 is specifically coupled to the unique inhibitory G protein subfamily member, G_z [7, 8]. The catalytic alpha subunit of G_z, $G\alpha_z$, is a canonical $G\alpha_i$ subfamily member, in that, when active, it binds to adenylate cyclase (AC) and inhibits the conversion of ATP to cAMP. Yet, $G\alpha_z$ has many characteristics that distinguish it from all of the other non-sensory-cell $G\alpha_{i/o}$ subfamily members. Notably, the GTP hydrolysis (i.e., inactivation) rate of $G\alpha_z$ is incredibly slow ($t_{1/2} \approx 10$ min)[31]. It has been estimated that up to 30% of $G\alpha_z$ molecules are active at any one time[31, 32]. In addition, of the 10 mammalian AC isoforms, $G\alpha_z$ has only been proven to have inhibitory activity towards AC1 and AC5, with activity towards AC6 being demonstrated *in vitro*[33]. Of note, AC1, AC5, and AC6 have all been shown as critical in GSIS and/or the adaptive response to obesity and insulin resistance[34-38]. Increased EP3 receptor expression, coupled with increased PGE_2 production, would set up a cycle where $G\alpha_z$ is chronically active, negatively influencing downstream GSIS and proliferation/survival pathways. The translational relevance of this concept is highlighted by recent work from our laboratory showing that over-expression of human $G\alpha_z$ in human donor islets reduces both insulin content and the insulin secretion response to stimulatory glucose, phenocopying results from islets isolated from T2D human organ donors[6, 30].

EP3-null BTBR-lean mice have normal 4-6 h fasting blood glucose levels, but are significantly more glucose intolerant than wild-type mice, even at 6 weeks of age (Fig. 2). Two previous studies have metabolically-phenotyped EP3-null mice. Ceddia and colleagues used a 16-week high-fat-diet regimen, initiated at 4 weeks of age, revealing a diet-dependent decrement in insulin sensitivity that was correlated with unregulated lipolysis, dyslipidemia, and systemic inflammation[12]. At 20 weeks of age, high-fat-diet fed EP3-null mice were significantly less glucose tolerant than their wild-type counterparts[12]. Sanchez-Alavez and colleagues maintained wild-type and EP3-null mice on breeder chow (approximately 20 kcal% fat, as compared to 10 kcal% fat in normal rodent chow) for 40 weeks, revealing EP3-null mice gradually became heavier than wild-type controls, developing hyperinsulinemia, hyperleptinemia, and worsening glucose tolerance between 3 and 6 months of age[39]. In both of these studies, the effect of EP3 loss on glucose tolerance was gradual and required a metabolic challenge. If one considers the underlying insulin resistance phenotype of the BTBR

strain, coupled with the exacerbation of insulin resistance resulting from systemic loss of EP3 (Figure 3), the rapid and significant effect of EP3 loss on lean BTBR mouse glucose tolerance is not unexpected.

Two underlying beta-cell defects have been previously identified in the BTBR mouse: a secretion defect and a proliferation defect. A SNP in the BTBR version of the *Stxbp5l* gene, encoding tomosyn-2, was found to be responsible for a diabetes susceptibility QTL in an F2 intercross between the BTBR-Ob and C57BL/6J Ob lines[2]. Tomosyn-2 is a negative regulator of SNARE complex formation and insulin granule exocytosis and is normally rapidly degraded after the beta-cell is exposed to stimulatory glucose. The BTBR tomosyn-2 variant appears relatively insensitive to this glucose-stimulated proteolytic degradation, significantly blunting second-phase GSIS[3]. Yet, tomosyn-2 protein degradation is also promoted by cAMP-stimulated phosphorylation, among other metabolic signals. In this study, we found expression of the constitutively-active EP3ɣ variant was also significantly up-regulated in islets BTBR-lean mice as compared to B6-lean (Figure 10B). The mechanism behind this up-regulation remains undetermined; yet, loss of $G\alpha_z$ in the BTBR beta-cell and relief of a tonic brake on cAMP production could certainly compensate for an underlying secretion defect, either through the classical mechanism(s) of PKA- and Rap1-mediated recruitment of insulin granules to the plasma membrane; targeting of tomosyn-2 for degradation; or both. The other beta-cell defect in BTBR mice is abnormal regulation of an islet gene module strongly associated with the cell cycle when mice are genetically obese[5]. This module is related to FoxM1 and its target genes, which have been linked with a proliferative response to pro-inflammatory cytokine stress[4]. With regards to an intrinsic, strain-specific proliferation defect in BTBR-lean islets, by interrogating a pre-existing microarray dataset, we found few changes in gene expression of FoxM1 or its target genes (Figure 8A,B), yet, we found cyclin D1 gene expression was significantly lower in BTBR islets than B6 islets at both 4 and 6 weeks of age (Figure 8C,D). Cyclin D1 expression is regulated by mitogenic and proliferative stimuli, and its expression is absolutely required in order for the cell to make the G1-to-S transition. One of the major transcriptional regulatory pathways for cyclin D1 is mediated by CREB. Upon consideration of the underlying insulin resistance of lean BTBR mice as a strain characteristic and a clear deficit in cyclin D1 expression at an age critical for “setting” baseline beta-cell mass, it is possible loss of $G\alpha_z$ and elevated cAMP production allows a proliferative response to mount, not only to classical beta-cell mitogens of the post-natal period, but also to insulin resistance itself. Our results of *Ccnd1* qPCR in islets from B6-lean, BTBR-lean, and $G\alpha_z$-null BTBR-lean mice were not strong enough to confirm the microarray results, but the lack of a significant effect of $G\alpha_z$ loss on BTBR-lean islet *Ccnd1* expression argues against increased proliferation as responsible for improved glucose tolerance (Fig. 9). This result does not exclude the possibility loss of beta-cell $G\alpha_z$ might up-regulate proliferation in conditions of severe glucolipotoxicity, where the ability of the beta-cell to replicate and survive becomes critical in maintaining euglycemia; yet, in this study, we were unable to test this hypothesis.

When islets are isolated from young, lean $G\alpha_z$-null mice or EP3-null mice, their islets secrete more insulin in response to stimulatory glucose, have a stronger incretin response, or both, with no effects of $G\alpha_z$ on beta-cell proliferation, whether measured directly (e.g., percentage of

nuclear Ki67-positive beta-cells; ^{3}H-thymidine incorporation) or by surrogate measurements (e.g., DNA content; protein content; insulin content; beta-cell fractional area; cyclin D1 mRNA expression) (Figures 6, 7 and [7, 9, 10]). A role for $G\alpha_z$ as a normal "check" on insulin secretion is highlighted by studies in 9-week-old wild-type and $G\alpha_z$-null BALB/c female mice. In the absence of $G\alpha_z$, BALB/c females have reduced blood glucose levels and accelerated glucose clearance[9]. Their islets secrete more insulin in response to stimulatory glucose, both *in vivo* and *ex vivo*, with no effect on islet protein content, DNA content, or insulin-positive area of pancreas sections[9]. When C57BL/6N or C57BL/6J mice lack $G\alpha_z$ throughout the body or specifically in the beta-cells, fasting blood glucose and glucose tolerance are unaffected ([7] and Supplemental Figure 5A,B). Yet, $G\alpha_z$-null C57BL/6N islets are more responsive to glucose and exendin-4 *ex vivo*, with no impact on insulin content or beta-cell fractional area [7]. When young, lean BTBR mice lack $G\alpha_z$ specifically in the beta-cells, they have no change in 4-6 h fasting blood or plasma glucose (Figure 2A and Supplemental Figure 5D) or fasting plasma insulin (Supplemental Figure 5E), but they are more responsive to glucose challenge (Figure 2C), and their islets secrete more insulin in response to exendin-4 (Figure 7). A pure secretion effect is supported by the lack of effect of beta-cell-specific $G\alpha_z$ loss on islet insulin content (Supplemental Figure 5F) or cyclin D1 mRNA expression (Figure 9). Finally, although EP3-null BTBR-lean mice are more insulin resistant than their wild-type controls (Figure 3), the major effect of EP3 loss on the islet phenotype is best explained by effects on secretion (Figure 6A-D). While EP3-null islets have lower insulin content (Figure 6E), this is consistent with their hypersecretory phenotype, and not a change in islet size, as quantified by insulin IHC (Figure 5).

The effect of $G\alpha_z$ (or EP3) loss on beta-cell phenotype is different than that observed in the lean, healthy state when mice are fed a HFD to induce obesity and insulin resistance. $G\alpha_z$-null C57BL/6N mice fed a high-fat-diet for 25-29 weeks, beginning at 11 weeks of age, secrete more insulin from their islets in response to stimulatory glucose, both *in vivo* and *ex vivo*, than wild-type controls, and are fully protected from developing diet-induced glucose intolerance[7]. Yet, this phenotype appears due solely to an increased replication response: islets from HFD-fed $G\alpha_z$-null C57BL/6N mice have the same deficits in GSIS as a percent of content as those from their wild-type counterparts—their islets secrete more insulin simply because they are bigger[7]. Both HFD-feeding and $G\alpha_z$ loss increase the percentage of Ki67-positive beta-cells as compared to wild-type C57BL/6N mice fed a control diet, but the loss of $G\alpha_z$ and HFD feeding is synergistic, suggesting the absence of $G\alpha_z$ removes a brake on the ability of the beta-cells to mount a compensatory replication response to HFD-induced insulin resistance and glucolipotoxicity[7]. Although studying the impact of HFD-feeding on the beta-cell phenotype of EP3-null C57BL/6J mice is compounded by the increased insulin resistance, inflammation, and glucolipotoxicity to which the beta-cells are exposed, islets from EP3-null C57BL/6J mice fed a HFD for 16 weeks, beginning at 4 weeks of age, similarly show no change in GSIS as a percent of content, yet have enhanced proliferation as compared to those from wild-type HFD-fed controls[12]. Taken together, the published results on the impact of EP3/$G\alpha_z$ loss on beta-cell function and beta-cell replication/mass in non-diabetic and T2D/glucolipotoxic mouse models fully supports both the importance of EP3 and $G\alpha_z$ in regulating key beta-cell signaling events that impact beta-cell biology and a divergence in these downstream signaling events depending on the physiologic conditions to which the beta-cell is exposed.

One explanation for the differing downstream effects of $G\alpha_z$ loss in the young, lean state vs. the T2D/glucolipotoxic state is that tonically-active $G\alpha_z$ and EP3 receptor-activated $G\alpha_z$ are two completely different molecules differing in three-dimensional structure based on the conformational change transmitted to $G\alpha_z$ by activated EP3. $G\alpha_z$ is unique in that, in its GTP-bound state, it can bind to Rap1GAP, a negative regulator of the small G protein, Rap1—a well-known contributor to the cAMP-mediated amplification pathway of GSIS and stimulator of cell proliferation pathways[40, 41]. Binding of $G\alpha_z$ to Rap1GAP and AC are mutually-exclusive[41]. In the classic model of G protein signaling, the Gα subunit, when GDP-bound and inactive, is complexed with Gβɣ and associated with a GPCR. When an agonist binds to the receptor, a conformational change occurs, allowing Gα to exchange GDP for GTP, releasing it from Gβɣ and the receptor, allowing both Gα and Gβɣ to signal to downstream effectors. The finding that mouse and human islet EP3 expression and/or function are primarily only up-regulated in the context of frank T2D/glucolipotoxicity provides circumstantial evidence for a model in which tonically-active $G\alpha_z$ and EP3 receptor-activated $G\alpha_z$ are two distinct molecules that preferentially bind either to AC isozymes or Rap1GAP, but not both. Yet, while Gβɣ is critical for regulating receptor-dependent Gα signaling, the Gα interaction with other proteins, including activator of G protein signaling (AGS) proteins, regulator of G protein signaling (RGS) proteins, myotubulin, and others, promotes receptor-independent Gα signaling. Furthermore, the function, activity, and/or abundance of $G\alpha_z$, Rap1GAP and other proteins involved in the EP3/$G\alpha_z$ signaling pathway are all altered by post-translational modifications (primarily phosphorylation) stimulated by cAMP- and/or inflammation-mediated signaling pathways[32, 42, 43]. $G\alpha_z$ phosphorylation status is activation-state-dependent and impacts its binding affinity for effector molecules[43]. With the importance of cAMP and inflammation in mediating beta-cell compensation, and, ultimately, beta-cell dysfunction and loss of functional beta-cell mass, it is likely that $G\alpha_z$ has preferential downstream signaling effects in different physiological milieus, not because of some intrinsic change in $G\alpha_z$ protein conformation when tonically-active vs. EP3 receptor-activated, but due to post-translational modifications promoted in these physiological milieus that impact $G\alpha_z$'s affinity for Gβɣ and other effectors/regulators. This overarching model is consistent not only with the results described in this manuscript, but with our entire previous body of work regarding the phenotype of $G\alpha_z$-null mice in various strain backgrounds; the physiological conditions (i.e., inflammatory, glucolipotoxic, or toxin-induced) behind development of hyperglycemia in wild-type mice; and the biological mechanisms (i.e., function, proliferation, and survival) underlying why $G\alpha_z$-null mice are protected from developing diabetes[7, 10, 11]. Proving this model is the subject of much current work.

Because we were not able to test the T2D resistance of a beta-cell-specific EP3-null mouse in the BTBR-Ob background, coupled with the importance of systemic EP3 in regulating lipolysis, the question remains open as to whether or how EP3 might be targeted therapeutically once an individual develops frank T2D, particularly as any constitutively-active EP3 isoform would be insensitive to traditional competitive antagonists. We also suspect, but cannot confirm, beta-cell $G\alpha_z$ loss and amplification of cAMP production corrects and/or compensates for underlying molecular defects that prohibit the BTBR beta-cell from mounting an appropriate insulin

secretion response, and that, were the islets to be stressed by severe insulin resistance, possibly underlying replication defects as well. Yet, even in the absence of this confirmation, our current results provide strong support for more research into how beta-cell $G\alpha_z$, either tonically-active or EP3-activated, might be targeted in individuals in the pre-diabetic state, whether this state is caused by an underlying genetic susceptibility or by the development of obesity and its often-associated systemic inflammation and insulin resistance.

5. Acknowledgements

We wish to thank the many present and former members of the Kimple Laboratory who contributed technical assistance or scientific discussion during the course of these experiments. This work was supported in part by Merit Review Award I01 BX003700-01A1 from the United States (U.S.) Department of Veterans Affairs Biomedical Laboratory Research and Development Service (BLR&D) (to M.E.K). The contents do not represent the views of the U.S. Department of Veterans Affairs or the United States Government. Further support was provided by ADA Grant 1-16-IBS-212 (to M.E.K.) and NIH Grant R01 DK102598 (to M.E.K). The funding bodies had no role in any aspect of the work described in this manuscript.

References

1. Clee, S.M., S.T. Nadler, and A.D. Attie, *Genetic and genomic studies of the BTBR ob/ob mouse model of type 2 diabetes.* Am J Ther, 2005. **12**(6): p. 491-8.
2. Bhatnagar, S., A.T. Oler, M.E. Rabaglia, D.S. Stapleton, K.L. Schueler, N.A. Truchan, et al., *Positional cloning of a type 2 diabetes quantitative trait locus; tomosyn-2, a negative regulator of insulin secretion.* PLoS Genet, 2011. **7**(10): p. e1002323.
3. Bhatnagar, S., M.S. Soni, L.S. Wrighton, A.S. Hebert, A.S. Zhou, P.K. Paul, et al., *Phosphorylation and degradation of tomosyn-2 de-represses insulin secretion.* J Biol Chem, 2014. **289**(36): p. 25276-86.
4. Davis, D.B., J.A. Lavine, J.I. Suhonen, K.A. Krautkramer, M.E. Rabaglia, J.M. Sperger, et al., *FoxM1 is up-regulated by obesity and stimulates beta-cell proliferation.* Mol Endocrinol, 2010. **24**(9): p. 1822-34.
5. Keller, M.P., Y. Choi, P. Wang, D.B. Davis, M.E. Rabaglia, A.T. Oler, et al., *A gene expression network model of type 2 diabetes links cell cycle regulation in islets with diabetes susceptibility.* Genome Res, 2008. **18**(5): p. 706-16.
6. Kimple, M.E., M.P. Keller, M.R. Rabaglia, R.L. Pasker, J.C. Neuman, N.A. Truchan, et al., *Prostaglandin E2 receptor, EP3, is induced in diabetic islets and negatively regulates glucose- and hormone-stimulated insulin secretion.* Diabetes, 2013. **62**(6): p. 1904-12.
7. Kimple, M.E., J.B. Moss, H.K. Brar, T.C. Rosa, N.A. Truchan, R.L. Pasker, et al., *Deletion of GalphaZ protein protects against diet-induced glucose intolerance via expansion of beta-cell mass.* J Biol Chem, 2012. **287**(24): p. 20344-55.
8. Kimple, M.E., A.B. Nixon, P. Kelly, C.L. Bailey, K.H. Young, T.A. Fields, et al., *A role for G(z) in pancreatic islet beta-cell biology.* J Biol Chem, 2005. **280**(36): p. 31708-13.
9. Kimple, M.E., J.W. Joseph, C.L. Bailey, P.T. Fueger, I.A. Hendry, C.B. Newgard, et al., *Galphaz negatively regulates insulin secretion and glucose clearance.* J Biol Chem, 2008. **283**(8): p. 4560-7.
10. Brill, A.L., J.A. Wisinski, M.T. Cadena, M.F. Thompson, R.J. Fenske, H.K. Brar, et al., *Synergy Between Galphaz Deficiency and GLP-1 Analog Treatment in Preserving Functional beta-Cell Mass in Experimental Diabetes.* Mol Endocrinol, 2016. **30**(5): p. 543-56.
11. Fenske, R.J., M.T. Cadena, Q.E. Harenda, H.N. Wienkes, K. Carbajal, M.D. Schaid, et al., *The Inhibitory G Protein alpha-Subunit, Galphaz, Promotes Type 1 Diabetes-Like Pathophysiology in NOD Mice.* Endocrinology, 2017. **158**(6): p. 1645-1658.
12. Ceddia, R.P., D. Lee, M.F. Maulis, B.A. Carboneau, D.W. Threadgill, G. Poffenberger, et al., *The PGE2 EP3 Receptor Regulates Diet-Induced Adiposity in Male Mice.* Endocrinology, 2016. **157**(1): p. 220-32.
13. Herrera, P.L., *Adult insulin- and glucagon-producing cells differentiate from two independent cell lineages.* Development, 2000. **127**(11): p. 2317-22.
14. Oropeza, D., N. Jouvet, L. Budry, J.E. Campbell, K. Bouyakdan, J. Lacombe, et al., *Phenotypic Characterization of MIP-CreERT1Lphi Mice With Transgene-Driven Islet Expression of Human Growth Hormone.* Diabetes, 2015. **64**(11): p. 3798-807.

15. Baan, M., K.J. Krentz, D.A. Fontaine, and D.B. Davis, *Successful in vitro fertilization and generation of transgenics in Black and Tan Brachyury (BTBR) mice.* Transgenic Res, 2016. **25**(6): p. 847-854.
16. Fenske, R.J. and M.E. Kimple, *Targeting dysfunctional beta-cell signaling for the potential treatment of type 1 diabetes mellitus.* Exp Biol Med (Maywood), 2018. **243**(6): p. 586-591.
17. Neuman, J.C., M.D. Schaid, A.L. Brill, R.J. Fenske, C.R. Kibbe, D.A. Fontaine, et al., *Enriching Islet Phospholipids With Eicosapentaenoic Acid Reduces Prostaglandin E2 Signaling and Enhances Diabetic beta-Cell Function.* Diabetes, 2017. **66**(6): p. 1572-1585.
18. Neuman, J.C., N.A. Truchan, J.W. Joseph, and M.E. Kimple, *A method for mouse pancreatic islet isolation and intracellular cAMP determination.* J Vis Exp, 2014(88): p. e50374.
19. Truchan, N.A., H.K. Brar, S.J. Gallagher, J.C. Neuman, and M.E. Kimple, *A single-islet microplate assay to measure mouse and human islet insulin secretion.* Islets, 2015. **7**(3): p. e1076607.
20. de Souza, A.H., L.R.B. Santos, L.P. Roma, M. Bensellam, A.R. Carpinelli, and J.-C. Jonas, *NADPH oxidase-2 does not contribute to β-cell glucotoxicity in cultured pancreatic islets from C57BL/6J mice.* Molecular and Cellular Endocrinology, 2017. **439**: p. 354-362.
21. Neuman, J.C. and M.E. Kimple, *The EP3 Receptor: Exploring a New Target for Type 2 Diabetes Therapeutics.* J Endocrinol Diabetes Obes, 2013. **1**(1).
22. Ichikawa, A., Y. Sugimoto, and S. Tanaka, *Molecular biology of histidine decarboxylase and prostaglandin receptors.* Proc Jpn Acad Ser B Phys Biol Sci, 2010. **86**(8): p. 848-66.
23. Kampmann, U., L.R. Madsen, G.O. Skajaa, D.S. Iversen, N. Moeller, and P. Ovesen, *Gestational diabetes: A clinical update.* World J Diabetes, 2015. **6**(8): p. 1065-72.
24. Butler, A.E., L. Cao-Minh, R. Galasso, R.A. Rizza, A. Corradin, C. Cobelli, et al., *Adaptive changes in pancreatic beta cell fractional area and beta cell turnover in human pregnancy.* Diabetologia, 2010. **53**(10): p. 2167-76.
25. Lillioja, S. and C. Bogardus, *Obesity and insulin resistance: lessons learned from the Pima Indians.* Diabetes Metab Rev, 1988. **4**(5): p. 517-40.
26. Ling, C., P. Poulsen, E. Carlsson, M. Ridderstrale, P. Almgren, J. Wojtaszewski, et al., *Multiple environmental and genetic factors influence skeletal muscle PGC-1alpha and PGC-1beta gene expression in twins.* J Clin Invest, 2004. **114**(10): p. 1518-26.
27. Maeda, R., I. Raz, F. Zurlo, and J. Sommercorn, *Activation of skeletal muscle casein kinase II by insulin is not diminished in subjects with insulin resistance.* J Clin Invest, 1991. **87**(3): p. 1017-22.
28. Poulsen, P., J.F. Wojtaszewski, I. Petersen, K. Christensen, E.A. Richter, H. Beck-Nielsen, et al., *Impact of genetic versus environmental factors on the control of muscle glycogen synthase activation in twins.* Diabetes, 2005. **54**(5): p. 1289-96.
29. DeFronzo, R.A. and D. Tripathy, *Skeletal muscle insulin resistance is the primary defect in type 2 diabetes.* Diabetes Care, 2009. **32 Suppl 2**: p. S157-63.
30. Truchan, N.A., H. Sandhu, R.J. Fenske, R. Buchanan, J. Moeller, A. Reuter, et al., *Differential Effects of Prostaglandin E2 Production and Signaling through the Prostaglandin EP3 Receptor on Human Beta-cell Compensation.* bioRxiv, 2019.

31. Casey, P.J., H.K. Fong, M.I. Simon, and A.G. Gilman, *Gz, a guanine nucleotide-binding protein with unique biochemical properties.* J Biol Chem, 1990. **265**(4): p. 2383-90.
32. Kimple, M.E., R.C. Hultman, and P.J. Casey, *Signaling through Gz*, in *Handbook of Cell Signaling, 2nd Edition*, R.A. Bradshaw and E. Dennis, Editors. 2009. p. 1649-1653.
33. Kimple, M.E. and D. Manning, *G protein alpha z.* UCSD Nature Molecule Pages, 1999.
34. Guenifi, A., G.M. Portela-Gomes, L. Grimelius, S. Efendic, and S.M. Abdel-Halim, *Adenylyl cyclase isoform expression in non-diabetic and diabetic Goto-Kakizaki (GK) rat pancreas. Evidence for distinct overexpression of type-8 adenylyl cyclase in diabetic GK rat islets.* Histochem Cell Biol, 2000. **113**(2): p. 81-9.
35. Halls, M.L. and D.M. Cooper, *Regulation by Ca2+-signaling pathways of adenylyl cyclases.* Cold Spring Harb Perspect Biol, 2011. **3**(1): p. a004143.
36. Hodson, D.J., R.K. Mitchell, L. Marselli, T.J. Pullen, S. Gimeno Brias, F. Semplici, et al., *ADCY5 couples glucose to insulin secretion in human islets.* Diabetes, 2014. **63**(9): p. 3009-21.
37. Parton, L.E., P.J. McMillen, Y. Shen, E. Docherty, E. Sharpe, F. Diraison, et al., *Limited role for SREBP-1c in defective glucose-induced insulin secretion from Zucker diabetic fatty rat islets: a functional and gene profiling analysis.* Am J Physiol Endocrinol Metab, 2006. **291**(5): p. E982-94.
38. Portela-Gomes, G.M. and S.M. Abdel-Halim, *Overexpression of Gs proteins and adenylyl cyclase in normal and diabetic islets.* Pancreas, 2002. **25**(2): p. 176-81.
39. Sanchez-Alavez, M., I. Klein, S.E. Brownell, I.V. Tabarean, C.N. Davis, B. Conti, et al., *Night eating and obesity in the EP3R-deficient mouse.* Proc Natl Acad Sci U S A, 2007. **104**(8): p. 3009-14.
40. Meng, J. and P.J. Casey, *Activation of Gz attenuates Rap1-mediated differentiation of PC12 cells.* J Biol Chem, 2002. **277**(45): p. 43417-24.
41. Meng, J., J.L. Glick, P. Polakis, and P.J. Casey, *Functional interaction between Galpha(z) and Rap1GAP suggests a novel form of cellular cross-talk.* J Biol Chem, 1999. **274**(51): p. 36663-9.
42. Hallak, H., L.F. Brass, and D.R. Manning, *Failure to myristoylate the alpha subunit of Gz is correlated with an inhibition of palmitoylation and membrane attachment, but has no affect on phosphorylation by protein kinase C.* J Biol Chem, 1994. **269**(6): p. 4571-6.
43. Fields, T.A. and P.J. Casey, *Phosphorylation of Gz alpha by protein kinase C blocks interaction with the beta gamma complex.* J Biol Chem, 1995. **270**(39): p. 23119-25.

Table 1: Primer Sequences and expected PCR product sizes for genotyping RIP-Cre-EP3-null and RIP-Cre-Gα_z-null lean and *Leptin^{Ob}* mice

Reaction	Primer Sequences	Band Size	allele
EP3-floxed	F: TCAACCTGCTAATCCCGCTG	424	deleted
	R: CAGTACCCGGCTTCTTAGGG	304	floxed
	ΔF: ACGTAACCCAAAGGCTGATGAG	194	wild-type
Gα_z-floxed	F: AAGGAACATCAGGGCCAGAG	581	floxed
	R: CAGCACTACGGTTCAGCAAC	461	wild-type
	ΔR: GGTCTTATGAACTGATGGCGAG	281	deleted
Cre Transgene	F: TGGTTTCCCGCAGAACCTGAAG	220	carrier
	R: GAGCCTGTTTTGCACGTTCACC	none	non-carrier
***Lep^{Ob}* mut.**	F: GGGCTTCACCCCATTCTGAG	104,44,14	mutant
	R: GGGAGCAGCTCTTGGAGAAG	144,14	wild-type

Table 2: Quantitative PCR primer sequences

Protein	Gene Symbol	Primer Sequences	Species Selectivity
Prostaglandin EP3 receptor (EP3)	*Ptger3*	F: GCTATCCCGCAGCTGAG R: CGCAGTCGTCGGTAGTAC	mouse
EP3ɣ splice variant		F: AGTTCTGCCAGGTAGCAAACG R: GCCTGCCCTTTCTGTCCAT	mouse
Cyclin D1	*Ccnd1*	F: CTGACACCAATCTCCTCAACGAC R: GCGGCCAGGTTCCACTTGAGC	mouse
β-actin	*Actb*	F: TCTTGGGTATGGAATCCTGTGGCA R: TCTCCTTCTGCATCCTGTCAGCAA	mouse

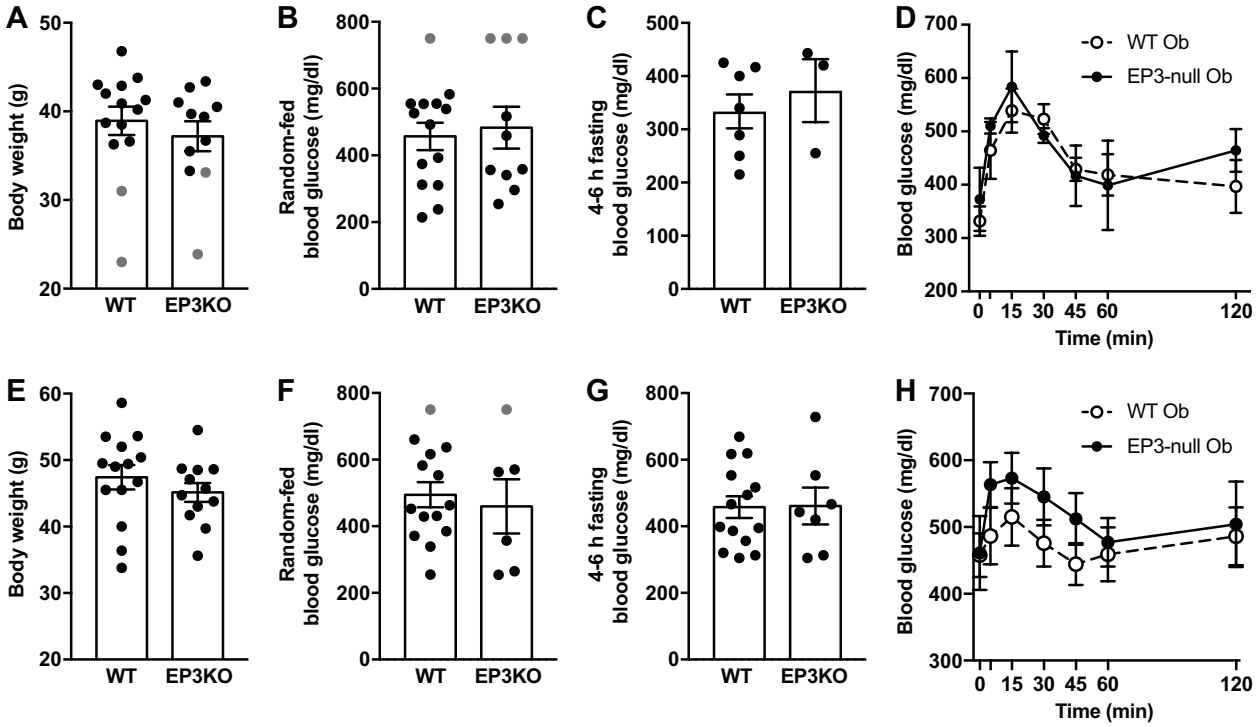

Figure 1: Full-body EP3 loss may accelerate the early T2D phenotype of BTBR-Ob mice. Male and female BTBR *Leptin^{Ob}* (Ob) mice were subjected to OGTT at 6 weeks of age and ITT at 8 weeks of age and relevant parameters recorded. A-D: 6-week body weights, random-fed blood glucose levels, 4-6 h fasting blood glucose levels, and glucose excursion after oral glucose challenge, respectively. In 'C' and 'D,' only mice without evidence of end-stage T2D and with 4-6 h FBG readings less than 450 mg/dl are reported. E-F: 8-week body weights, random-fed blood glucose levels, 4-6 h fasting blood glucose levels, and glucose excursion after IP insulin challenge, respectively. Grey circles in 'A' indicate mice that had begun losing weight, presumably as a factor of end-stage T2D. Grey circles at 750 mg/dl in 'B' and 'F' indicate blood glucose readings above the range of the glucometer. Body weights and fasting blood glucose were compared by t-test. Blood glucose levels over time were compared by 2-way paired ANOVA, with Sidak test post-hoc to correct for multiple comparisons. No significant differences between means were found with any comparison.

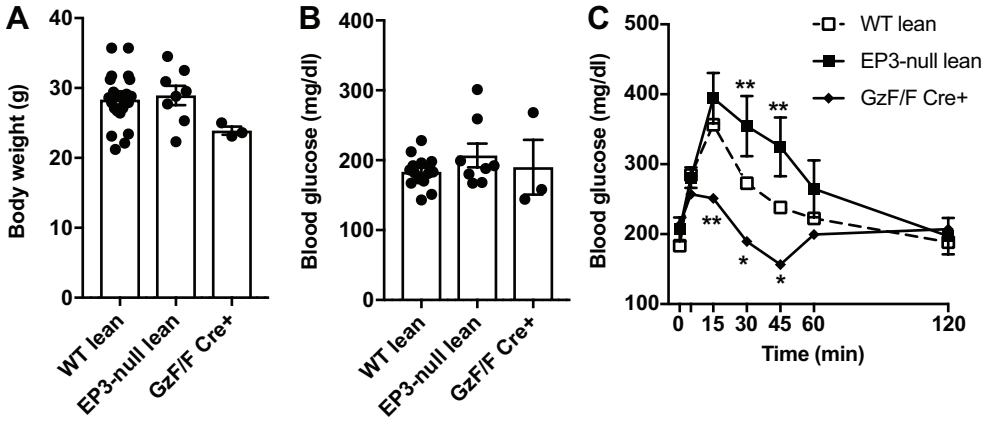

Figure 2. Full-body EP3 loss promotes glucose intolerance in 6-week-old BTBR-lean mice, while beta-cell-specific $G\alpha_z$ loss accelerates glucose clearance. Male and female BTBR-lean mice were subjected to OGTT at 6 weeks of age and relevant parameters recorded. A-C: 6-week body weights, 4-6 h fasting blood glucose levels, and glucose excursion after oral glucose challenge, respectively. The WT lean and EP3-null lean groups contained both Cre-negative and Cre-positive animals, as Cre expression had no impact on metabolic parameters of interest (see Supplemental Figure 4). Body weights and fasting blood glucose were compared by t-test. Blood glucose levels over time were compared by 2-way paired ANOVA, with Sidak test post-hoc to correct for multiple comparisons. *, $p < 0.05$ and **, $p < 0.01$ vs. the wild-type lean control group. If no p value is indicated, the difference in means was not statistically significant.

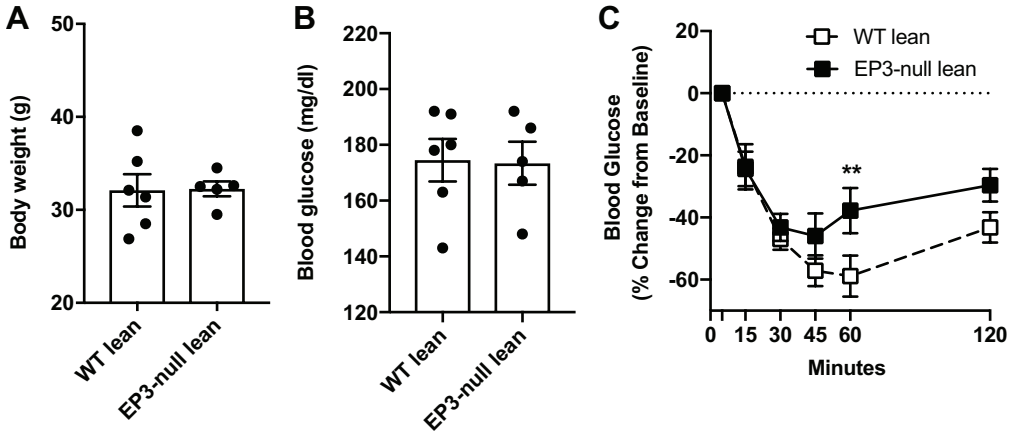

Figure 3: Full-body EP3 loss promotes insulin resistance in 8-week-old BTBR-lean mice. Male and female wild-type and EP3-null BTBR lean mice were subjected to ITT at 8 weeks of age and relevant parameters recorded. A-C: 8-week body weights, 4-6 h fasting blood glucose levels, and percent change in blood glucose levels from baseline after IP insulin challenge. Body weights and fasting blood glucose were compared by t-test. Percent decrement in blood glucose over time was compared by 2-way paired ANOVA, with Sidak test post-hoc to correct for multiple comparisons. **, $p < 0.01$ vs. the indicated control group. If no p value is indicated, the difference in means was not statistically significant.

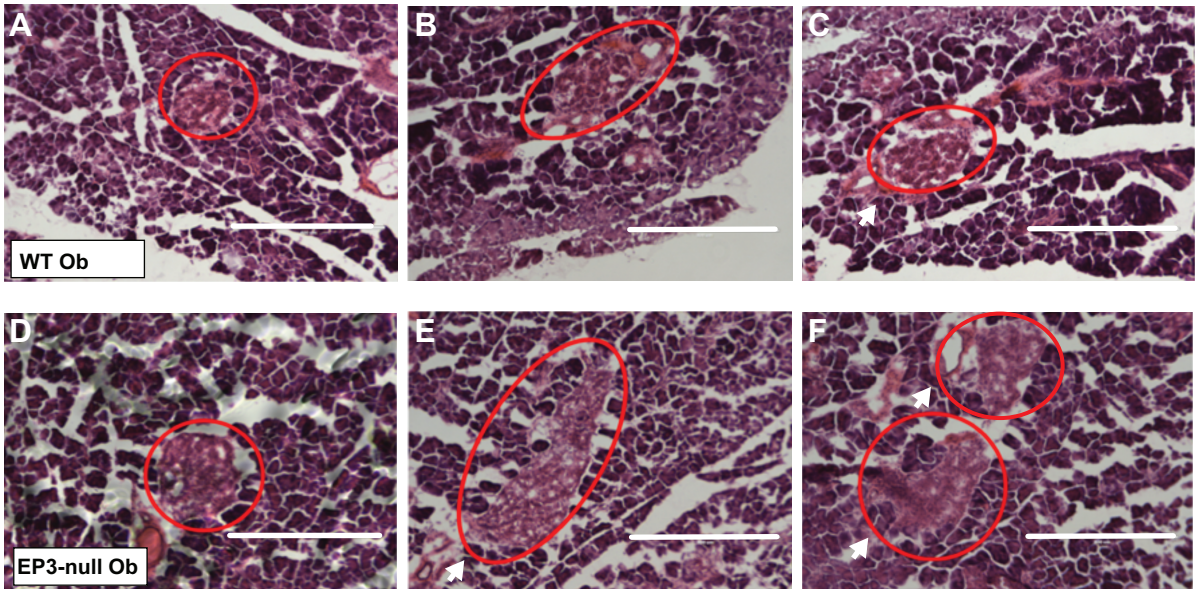

Figure 4: Loss of normal pancreatic islet architecture in 9-10-week old wild-type and EP3-null BTBR-Ob mice. Paraffin-embedded, fixed pancreas sections from 9-10-week old wild-type and EP3-null BTBR-Ob mice were stained with hematoxylin and eosin for morphometric visualization of islet architecture. Three representative images per genotype are shown (wild-type BTBR-Ob, panels A-C; EP3-null BTBR-Ob, panels D-F). In each image, an islet or islet remnant is circled in red. While islet morphology was not quantified, qualitative analysis suggested more islets with poor morphology in EP3-null BTBR-Ob mice (white arrowheads). Scale bars = 1000 µm.

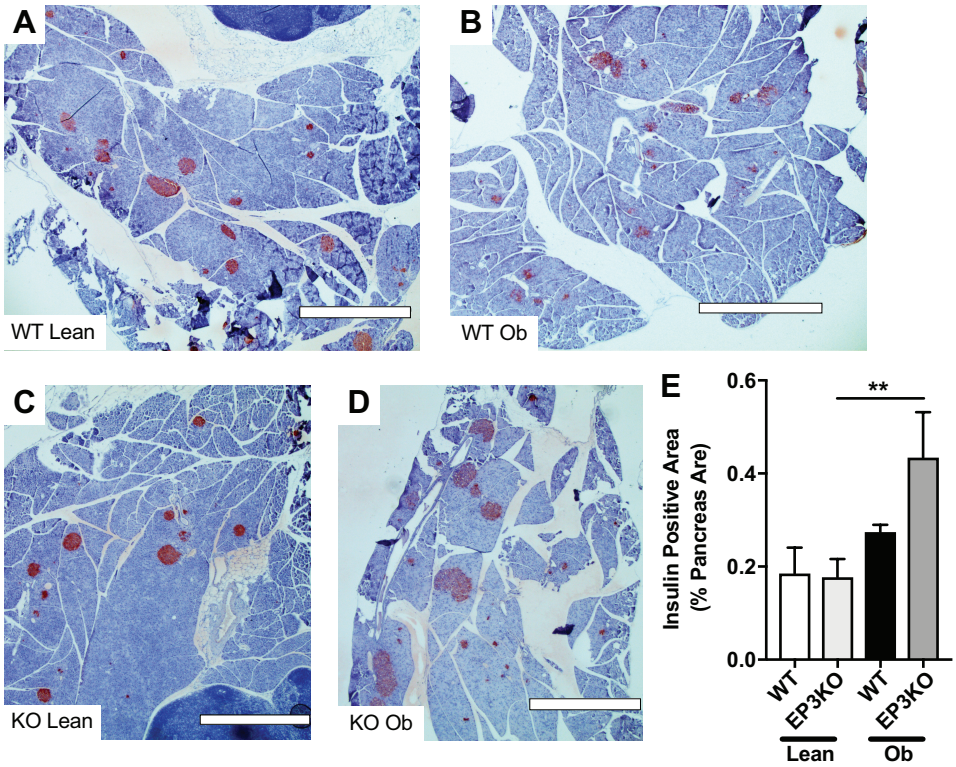

Figure 5: Insulin-positive pancreas area is not significantly affected by the EP3-null mutation in BTBR-lean or BTBR-Ob mice. Paraffin-embedded, fixed pancreas sections from 9-10-week old wild-type and EP3-null BTBR-Ob mice were subject to insulin immunohistochemical staining, followed by hematoxylin counter-staining in order to quantify insulin-positive pancreas area as a function of total pancreas area. Representative images from wild-type (WT) BTBR-lean, WT BTBR-Ob, EP3-null (KO) BTBR-lean, and KO BTBR-Ob are shown in panels A-D, respectively. E: Quantification of results from two pancreas sections separated by 200 µm least 3 mice of each genotype. Data in E were compared by two-way ANOVA with Tukey's test post-hoc. **, $p < 0.01$. Scale bars = 1000 µm.

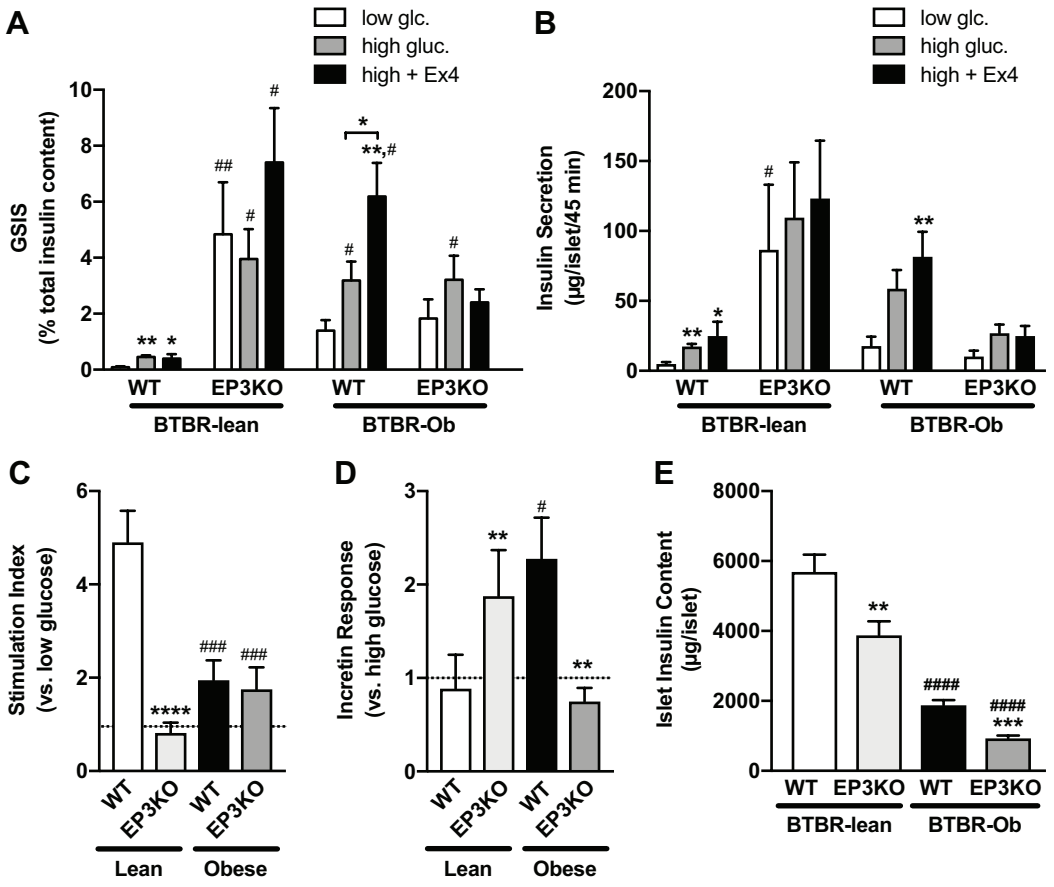

Figure 6: Pancreatic islets from EP3-null mice have dysfunctional insulin secretion in response to non-stimulatory and stimulatory concentrations of glucose. Islets were isolated from at least 3 mice of each genotype and subjected to single-islet GSIS assays in 1.7 mM glucose (low), 16.7 mM glucose (high), and 16.7 mM glucose plus 10 nM exendin-4 (high + Ex4). Data are represented as the percent insulin secreted as normalized to islet insulin content (A), µg of insulin secreted per islet over 45 min (B) GSIS in high glucose over low glucose (stimulation index) (C), GSIS in high glucose + Ex4 over high glucose (incretin response) (D) and average islet insulin content (E). For 'A' and 'B', within-group data analysis (groups: BTBR-lean and BTBR-Ob) was first performed by ordinary one-way ANOVA with Sidak test post-hoc to correct for multiple comparisons. *, $p < 0.05$ and **, $p < 0.01$ vs. the insulin secreted in 1.7 mM glucose within each group. $^{\#}$, $p < 0.05$ and $^{\#\#}$, $p < 0.01$ vs. the appropriate stimulation condition in WT-lean islets. In 'C,' 'D,' and 'E,' both intra-group and inter-group analyses were performed by unpaired t-test. **, $p < 0.01$, ***, $p < 0.001$, and ****, $p < 0.0001$ to WT control within groups. $^{\#}$, $p < 0.05$, $^{\#\#\#}$, $p < 0.001$, and $^{\#\#\#}$, $p < 0.0001$ vs. the value for WT BTBR-lean between groups. N ≥ 5 independent measurements in 'A' through 'D.' N ≥ 32 independent measurements in 'E.' If a p-value is not indicated, the difference in means was not statistically significant.

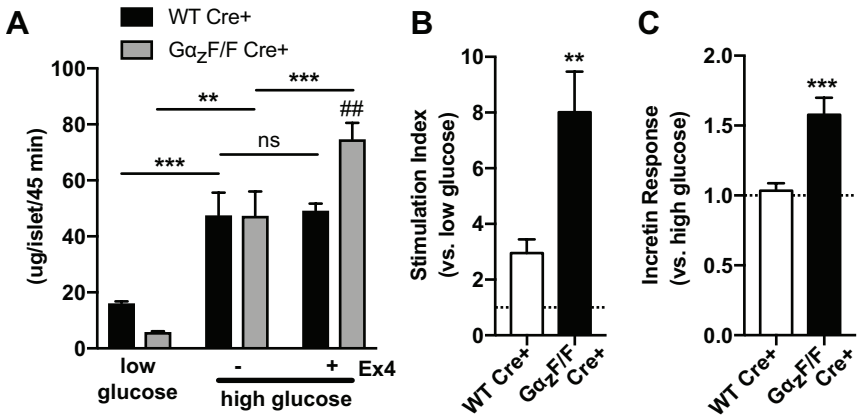

Figure 7. Pancreatic islets from a BTBR lean mouse lacking beta-cell Gα$_z$ have significantly increased responsiveness to exendin-4. Islets were isolated from one RIP-Cre- Gα$_z$-floxed BTBR-lean mouse and one wild-type Cre-positive control and subject to single-islet GSIS assays in 1.7 mM glucose (low), 16.7 mM glucose (high), and 16.7 mM glucose plus 10 nM exendin-4 (high + Ex4). Data are represented as the µg of insulin secreted per islet over 45 min (A), ratio of insulin secreted in high glucose over low glucose (stimulation index) (B), and ratio of insulin secreted in high glucose + Ex4 over high glucose (incretin response) (C) In 'A,' within-group and inter-group data analyses were performed by ordinary one-way ANOVA with Sidak test post-hoc to correct for multiple comparisons. *, $p < 0.05$, **, $p < 0.01$, and ***, $p < 0.001$ vs. the indicated control. $^{##}$, $p < 0.01$ vs. insulin secreted in wild-type Cre-positive islets in high glucose + exendin 4. In 'B' and 'C,' analyses were performed by unpaired t-test. **, $p < 0.01$ and ***, $p < 0.001$ vs. wild-type control islets. Data are representative of measurements from at least 12 islets per group per treatment condition. If a p-value is not indicated, the difference in means was not statistically significant.

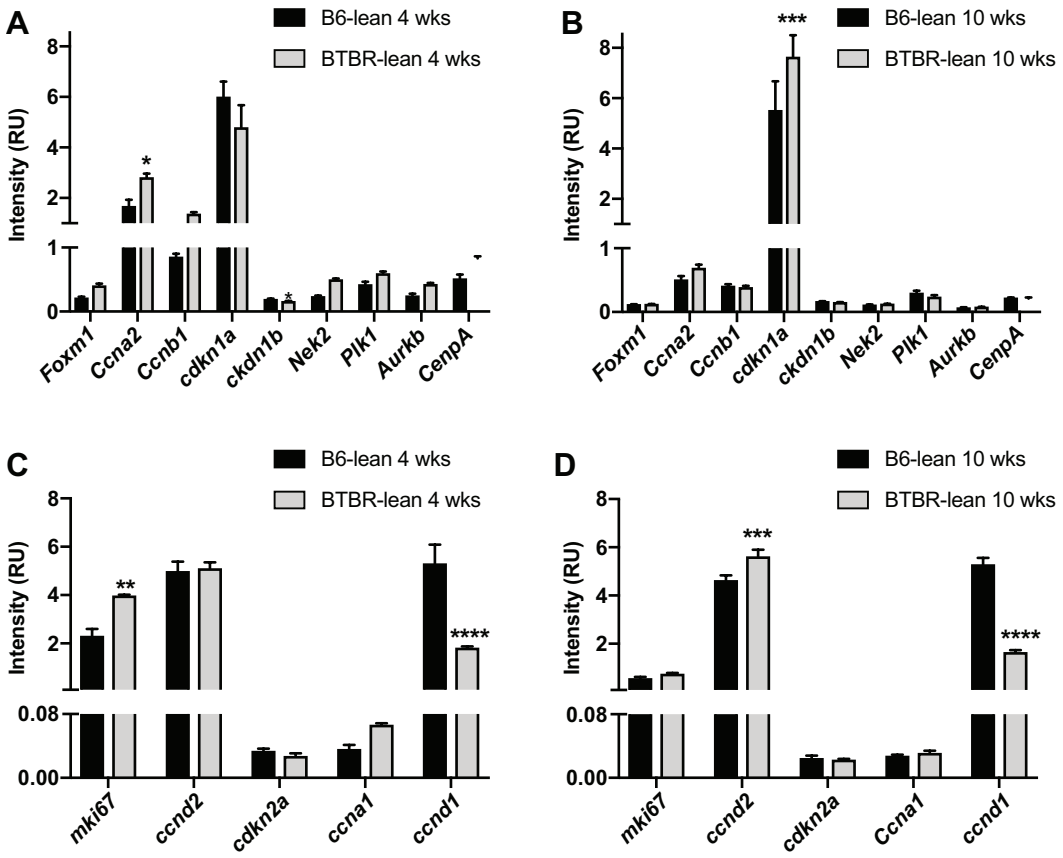

Figure 8. Few changes in expression of cell cycle regulatory genes are observed in BTBR-lean vs. B6-lean islets at 4 or 10 weeks of age. We interrogated a publicly-available microarray database of islet gene expression in C57BL/6J and BTBR mice at 4 and 10 weeks of age (diabetes.wisc.edu, [5]), to search for expression changes in key cell cycle genes by strain background. The intensity data from each biological replicate (N=5/group) was downloaded and plotted in GraphPad Prism in order to perform statistical analyses. A and B: FoxM1 and select target genes. D and E: Other select cell cycle genes not regulated by FoxM1. Statistical analyses were performed by t-test. *, $p < 0.05$, **, $p < 0.01$, ***, $p < 0.001$, and ****, $p < 0.0001$ vs. B6-lean. If a p-value is not indicated, the difference in means was not statistically significant.

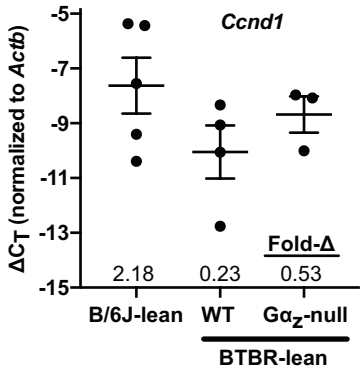

Figure 9. BTBR-lean islet Cyclin D1 mRNA expression is unaffected by $G\alpha_z$ loss. qPCR was performed in cDNA samples from islets of 10-week-old B6-lean and BTBR-lean (both wild-type and $G\alpha_z$-null) using primers specific for β-actin mRNA (*Actb*) and cyclin D1 mRNA (*Ccnd1*). Data are represented as ΔC_T as normalized to Actb, and the fold-change in mRNA abundance as compared to B6-lean (as calculated via the $2^{\Delta\Delta Ct}$ method indicated above the X-axis labels (Fold-Δ). ΔC_T values were compared by both one-way ANOVA (all three groups) and t-test (WT vs. $G\alpha_z$-null BTBR-lean). No significant differences among any of the means were observed.

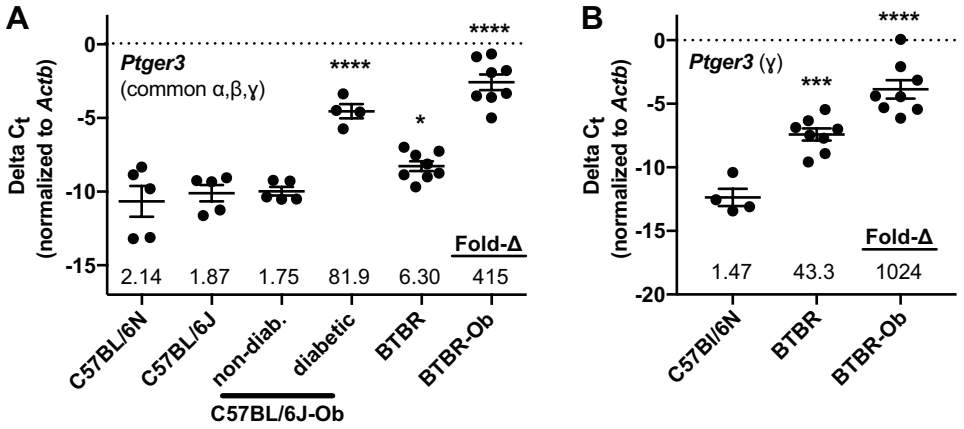

Figure 10. Total EP3 mRNA and EP3ɣ splice variant mRNA abundance are differentially expressed in isolated islets by strain background and T2D status. A) qPCR was performed in cDNA samples of islets isolated from 10-week-old C57Bl/6N, C57Bl/6J, C57BL/6J-Ob (both euglycemic and T2D: 4-6 h FBG > 450 mg/dl), BTBR, and BTBR-Ob (all T2D) using a primer set that recognizes all three mouse EP3 splice variants (*Ptger3* α, β, ɣ), and C_T values normalized to those of β-actin (*Actb*). While T2D status significantly up-regulates *Ptger3* expression regardless of C57BL/6J or BTBR strain background, of the lean mouse strains, only islets from BTBR mice have significantly enhanced *Ptger3* expression as compared to C57BL/6N controls. B) Primers specific for the constitutively-active EP3ɣ splice variant were used in a subset of strains from 'A,' revealing significantly increased EP3ɣ mRNA expression in islets from BTBR-lean mice as compared to C57BL/6N, with an even greater increase in islets isolated from T2D BTBR-Ob mice. In both 'A' and 'B,' ΔC_T values were compared by one-way ANOVA with Bonferroni's test post-hoc using C57BL/6N islets as the control group. The fold-change in mRNA abundance as compared to C57Bl/6N was determined via the $2^{\Delta\Delta Ct}$ method and is indicated above the X-axis labels (Fold-Δ). *, $p < 0.05$, ***, $p < 0.001$, and ****, $p < 0.0001$ vs. C57BL/6N. If a p-value is not indicated, the difference in means was not statistically significant.

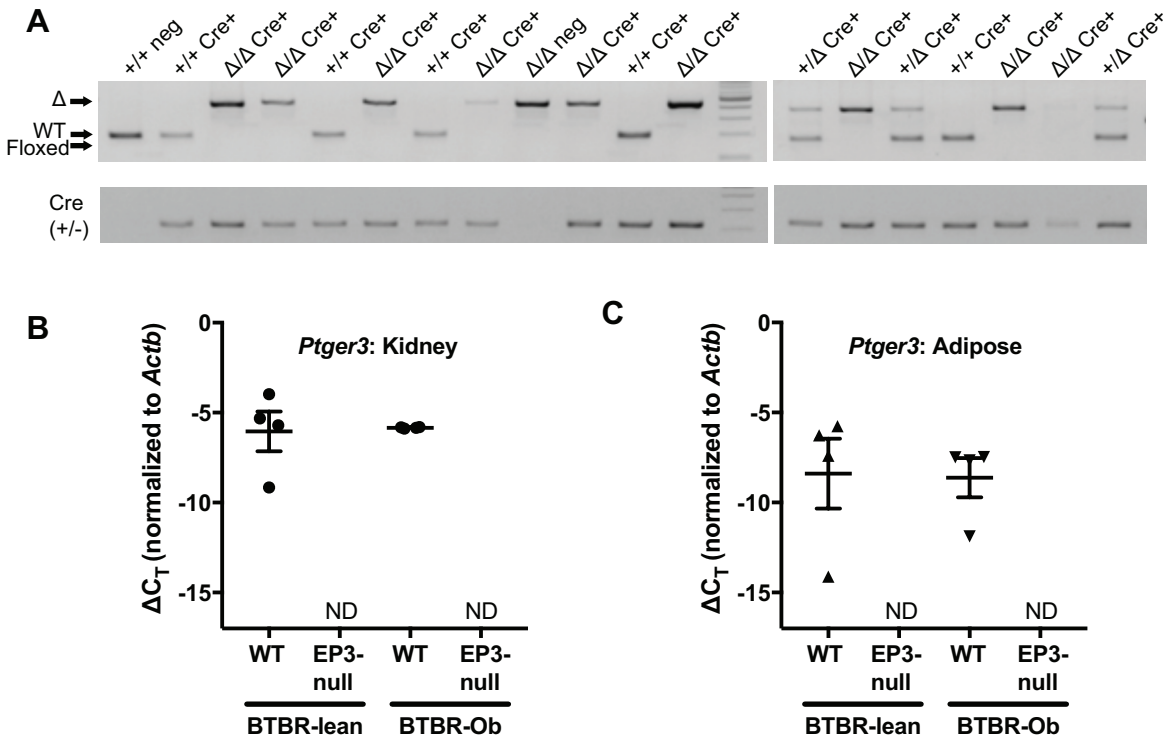

Supplemental Figure 1. Confirmation of germline transmission of the EP3-floxed deleted allele and generation of a full-body EP3-null BTBR mouse. A: Genotyping results from ear punches showing only the wild-type or deleted allele, and not the floxed allele, in all genotyping reactions, regardless of Cre expression. B and C: qPCR results using primers specific for all three mouse EP3 splice variants in kidney and adipose tissue: two tissues with high endogenous EP3 expression. In neither case was *Ptger3* detected in EP3-null mouse tissue samples.

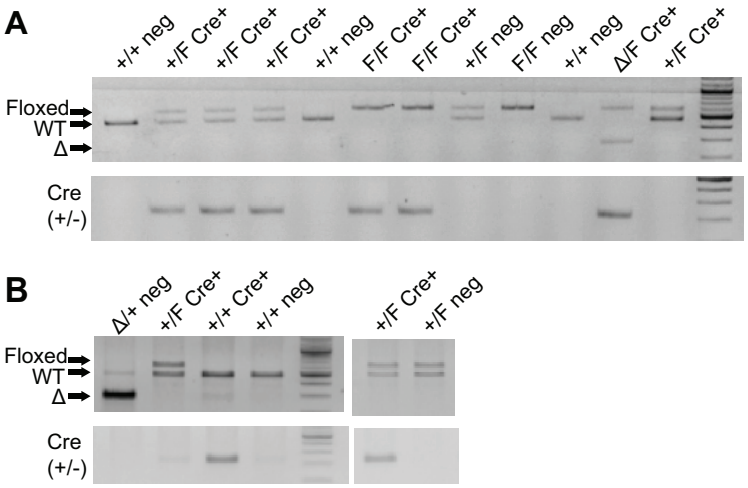

Supplemental Figure 2. Confirmation of non-germline transmission of the Gα$_z$-floxed deleted allele in the BTBR and C57BL/6J line. Genotyping results from ear punches from (A) BTBR mice and (B) C57BL/6J mice showing the occasional appearance of the Gα$_z$-floxed deleted allele, which is easily distinguished from the wild-type and floxed alleles. Progeny showing a deleted allele were humanely euthanized.

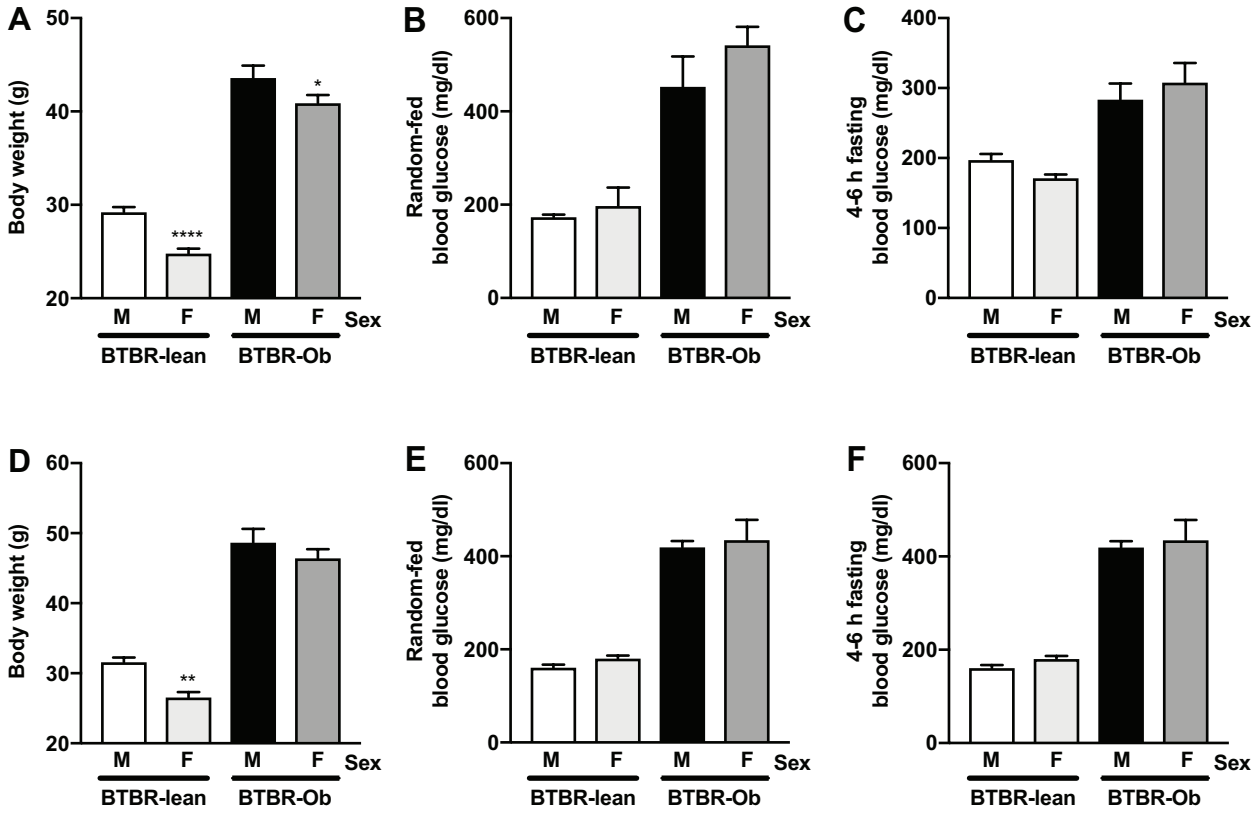

Supplemental Figure 3. Although females are lighter, sex has no impact on random-fed or 4-6 h fasting blood glucose levels at 6 or 8 weeks of age in the BTBR strain, whether lean or obese. A-C: 6-week body weights, random-fed blood glucose levels, or 4-6 h fasting blood glucose levels, respectively, of BTBR-lean or BTBR-Ob mice segregated by sex. D-E: 8-week body weights, random-fed blood glucose levels, or 4-6 h fasting blood glucose levels, respectively, of BTBR-lean or BTBR-Ob mice segregated by sex. Male and female data within groups were compared by t-test. *, $p < 0.05$, **, $p < 0.01$, and ****, $p < 0.0001$ vs. male.

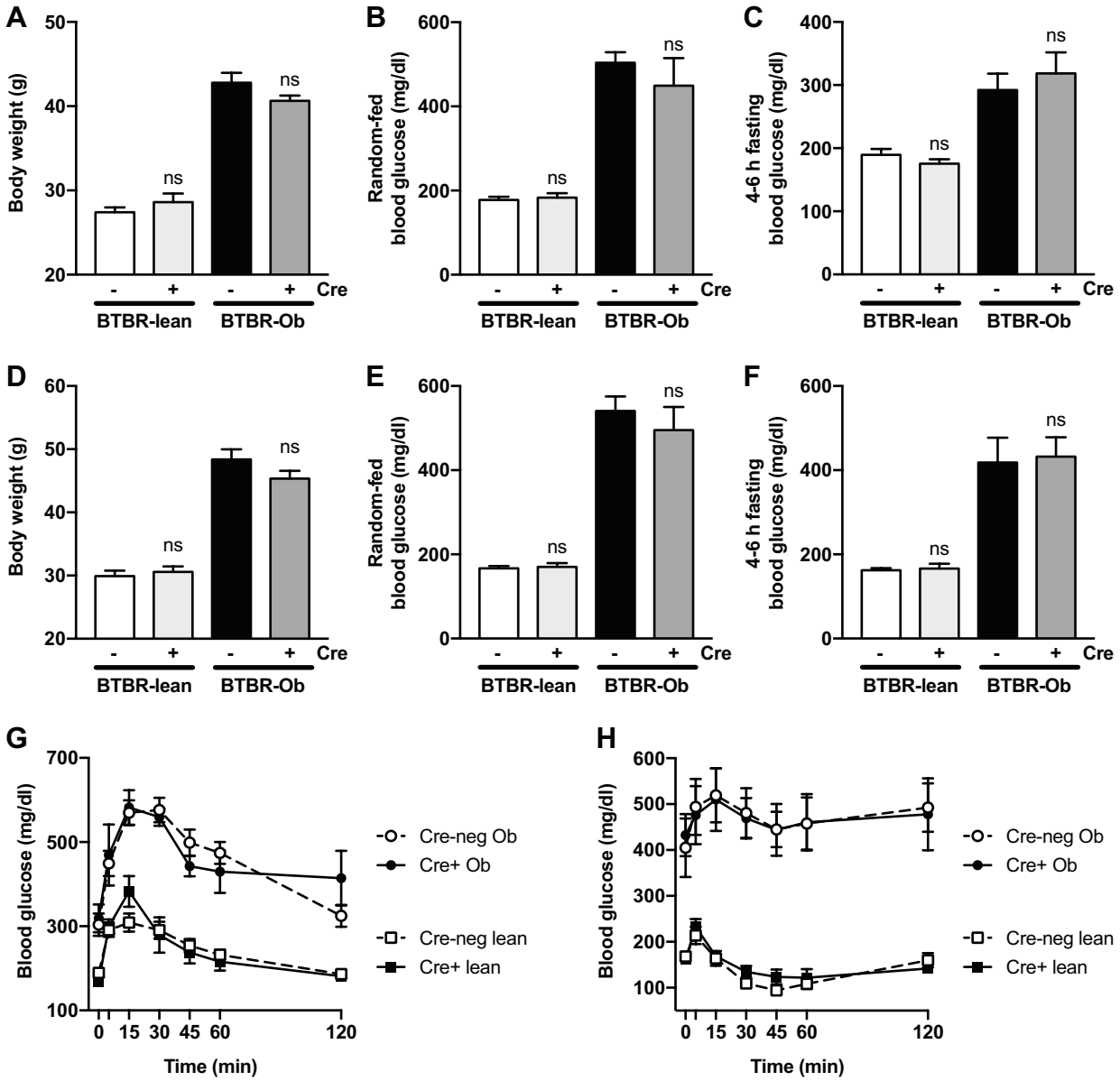

Supplemental Figure 4. Beta-cell Cre expression has no impact on metabolic parameters of 6- or 8-week-old BTBR lean or Ob mice. A-C: 6-week body weights, random-fed blood glucose levels, or 4-6 h fasting blood glucose levels, respectively, of BTBR-lean or BTBR-Ob mice segregated by Cre expression. D-E: 8-week body weights, random-fed blood glucose levels, or 4-6 h fasting blood glucose levels, respectively, of BTBR-lean or BTBR-Ob mice segregated by Cre expression. G: Blood glucose excursion curves after oral glucose challenge of 6-week-old BTBR-lean or Ob mice, both Cre-negative and Cre-positive. H: Blood glucose excursion curves after IP insulin challenge of 8-week-old BTBR-lean or Ob mice, both Cre-negative and Cre-positive. In A-F, Cre-negative and Cre-positive data within groups were compared by t-test. In G and H, Cre-negative and Cre-positive data within groups were compared by two-way ANOVA with Sidak's test post-hoc. None of the statistical analyses revealed any significant differences in means as a factor of beta-cell Cre expression.

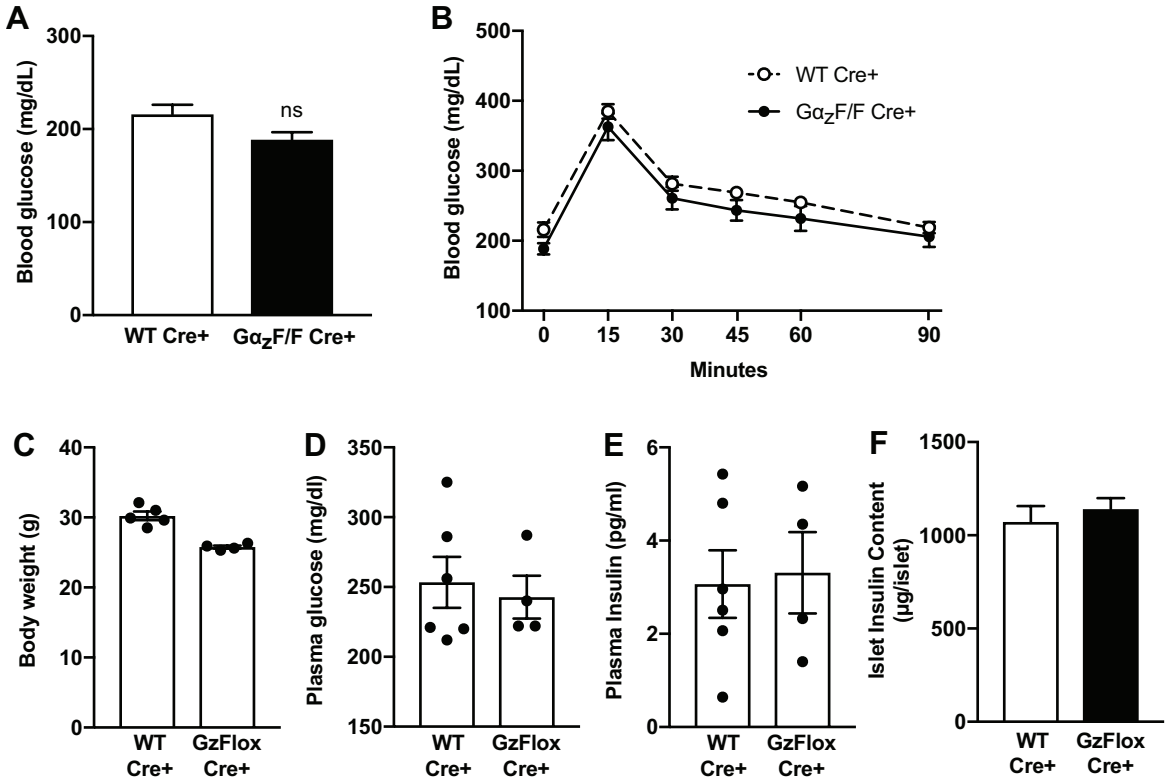

Supplemental Figure 5. Beta-cell-specific $G\alpha_z$ loss has no impact on glucose tolerance of 10-week-old C57BL/6J mice, and does not impact baseline metabolic/islet parameters of 10-week-old BTBR-lean mice. A and B: 10-week-old male C57BL/6J mice (N=10/group), either wild-type Cre-positive or RIP-Cre-$G\alpha_z$-floxed, were fasted 4-6 h prior to oral glucose challenge. 4-6 h fasting blood glucose levels are shown in 'A' and glucose excursion after OGTT in 'B.' C-F: 10-week-old BTBR-lean mice, either wild-type Cre-positive or RIP-Cre-$G\alpha_z$-floxed, were fasted 4-6 h prior to terminal blood collection and islet harvest. There were no differences by genotype in body weight (A), plasma glucose (B), plasma insulin (C), or mean islet insulin content (F). In A and C-F, statistical analyses were performed by t-test. In B, statistical analyses were performed by 2-way paired ANOVA, with Sidak test post-hoc to correct for multiple comparisons. In all panels, if no p value is indicated, the difference in means was not statistically significant.

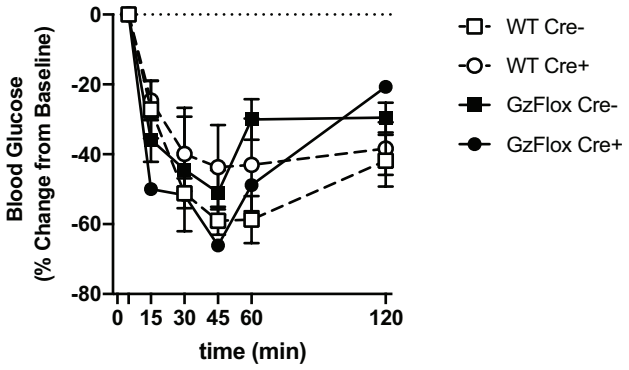

Supplemental Figure 6. Beta-cell-specific Gα_z loss likely has no impact on insulin sensitivity of 8-week-old BTBR-lean mice. 8 week-old male and female BTBR-lean mice, either wild-type Cre-negative (N=4), wild-type Cre-positive (N=5), Gα_z-floxed Cre-negative (N=2) or Gα_z-floxed Cre-positive (N=1) were fasted for 4-6 h prior to insulin challenge and blood glucose levels recorded over time. Data are represented as the percent decrease in blood glucose levels from their baseline value. Although with only one Gα_z-floxed Cre-positive mouse, a statistical analysis was not performed, all of the mean insulin tolerance curves essentially overlay each other.